Eur. Phys. J. C (2023) 83:638
https://doi.org/10.1140/epjc/s10052-023-11808-0

THE EUROPEAN PHYSICAL JOURNAL C

Regular Article - Theoretical Physics

A minimal axion model for mass matrices with five texture-zeros

Yithsbey Giraldo[1,a], **R. Martinez**[2,b], **Eduardo Rojas**[1,c], **Juan C. Salazar**[1,d]

[1] Departamento de Física, Universidad de Nariño, A.A. 1175 San Juan de Pasto, Colombia
[2] Departamento de Física, Universidad Nacional de Colombia, Ciudad Universitaria, K.45 No. 26-85, Bogota D.C., Colombia

Received: 24 April 2023 / Accepted: 5 July 2023 / Published online: 19 July 2023
© The Author(s) 2023

Abstract A model with fermion and scalar fields charged under a Peccei–Queen (PQ) symmetry is proposed. The PQ charges are chosen in such a way that they can reproduce mass matrices with five texture zeros, which can generate the fermion masses, the CKM matrix, and the PMNS matrix of the Standard Model (SM). To obtain this result, at least 4 Higgs doublets are needed. As we will see in the manuscript this is a highly non-trivial result since the texture zeros of the mass matrices impose a large number of restrictions. This model shows a route to understand the different scales of the SM by extending it with a multi-Higgs sector and an additional PQ symmetry. Since the PQ charges are not universal, the model predicts flavor-changing neutral currents (FCNC) at the tree level, a feature that constitutes the main source of restrictions on the parameter space. We report the allowed regions by lepton decays and compare them with those coming from the semileptonic decays $K^{\pm} \longrightarrow \pi \bar{\nu} \nu$. We also show the excluded regions and the projected bounds of future experiments for the axion–photon coupling as a function of the axion mass and compare it with the parameter space of our model.

1 Introduction

The discovery of the Higgs with a mass of 125 GeV, by the ATLAS [1] and CMS [2] collaborations, is very important because it provides experimental support for spontaneous symmetry breaking, which is the mechanism that explains the origin of the masses of fermions and gauge bosons. Additionally, it opens up the possibility of new physics in the scalar sector, such as the two Higgs doublet model [3–7], models with additional singlet scalar fields [8–10], or scalar fields that could be candidates for Dark Matter [11–14]. On the other hand, in the Standard Model (SM) [15–17], symmetry breaking generates a coupling of the Higgs to fermions, proportional to their masses, which is consistent with experimental data. However, there are several orders of magnitude between the fermion mass hierarchies that cannot be explained within the context of the SM. Six masses must be defined for the up and down quarks, three Cabibbo-Kobayashi-Maskawa (CKM) mixing angles, and a complex phase that involves CP violation. On the other hand, in the lepton sector, there are three masses for charged leptons, two squared mass differences for neutrinos, three mixing angles, and a complex phase that involves CP violation in the lepton sector. In this case, it is necessary to determine the mass of the lightest neutrino and the character of neutrinos, whether they are Dirac or Majorana fermions.

In the Davis experiment [18], which was designed to detect solar neutrinos, a deficiency in the solar neutrino flux was first observed. According to the results of Bahcall, only one-third of solar neutrinos would reach the Earth [19]. Neutrino oscillation was first proposed by Pontecorvo [20], and the precise mechanism of solar neutrino oscillations was proposed by Mikheyev, Smirnov, and Wolfenstein, involving a resonant enhancement of neutrino oscillations due to matter effects [21,22]. These observations have been confirmed by many experiments from four different sources: solar neutrinos as in Homestake [18], SAGE [18], GALLEX & GNO [23,24], SNO [25], Borexino [26,27] and Super-Kamiokande [28,29] experiments, atmospheric neutrinos as in IceCube [30], neutrinos from reactors as KamLAND [31], CHOOZ [32], Palo Verde [33], Daya Bay [34], RENO [35] and SBL [36], and from accelerators as in MINOS [37], T2K [38] and NOνA [39]. Neutrino oscillations depend on squared mass differences. On the other hand, the lightest neutrino mass has not been determined yet, but from cosmological considerations, none of the neutrino masses can exceed 0.3 eV, which implies

[a] e-mail: yithsbey@gmail.com
[b] e-mail: remartinezm@unal.edu.co
[c] e-mail: eduro4000@gmail.com
[d] e-mail: jusala@gmail.com (corresponding author)

that the neutrino masses are much smaller than the charged fermion masses. However, unlike quarks and charged leptons, in the SM the neutrinos are massless, which is explained by assuming that neutrinos are left-handed. Therefore, the discovery of neutrino masses implies new physics beyond the SM. By adding right-handed neutrinos, the Higgs mechanism of the SM can give neutrinos the same type of mass acquired by charged leptons and quarks. It is possible to add right-handed neutrinos ν_R to the SM, as long as they do not participate in weak interactions. With the presence of right-handed neutrinos, it would be possible to generate Dirac masses m_D, similar to those of charged leptons and quarks. In principle, it is also possible to give Majorana masses to left-handed neutrinos, and similarly, right-handed neutrinos can have Majorana masses M_R. For a very large M_R, it would give effective Majorana masses for left-handed neutrinos as $m_{\text{eff}} \approx m_D^2/M_R$. The presence of large Majorana masses allows to explain the tiny neutrino masses compared to the charged fermion masses [38]. To explain the smallness of neutrino masses, there are three types of seesaw mechanisms in the literature: type I with three electroweak neutrinos and three heavy right-handed neutrinos, type II [40,41], type III [42], and inverse seesaw [43,44]. One way to explain the fermion mass hierarchies and the CKM and PMNS mixing angles is through zeros in the Yukawa couplings of fermions (this is known as texture-zeros or simply textures of the mass matrices, and these zeros are usually chosen by hand). It is common in the literature to consider Fritzsch-type textures [45,46], or similar [47–52], for the neutrino and charged lepton mass matrices.

There is no theory that provides values for the entries of the Yukawa Lagrangian, and consequently, there is no a first-principle explanation for the masses and their large differences in the SM. The mass hierarchy between fermions is unnatural because it requires Yukawa constants that differ by many orders of magnitude; this feature is known as the flavor problem or flavor puzzle [53–57]. In this direction, a way that has been explored in the literature is to propose a sector with multiple scalar doublets along with discrete symmetries [58,59], to reduce the number of Yukawa couplings, or equivalently, by introducing texture-zeros in the mass matrices [60–65]. It is also possible to consider global symmetry groups that prohibit certain Yukawas, which somehow generate the texture-zeros mentioned [53–57]. Another way of obtaining these textures is through horizontal gauge symmetries, with the assignment of quantum numbers to the fermion sector, which can break the universality of the SM [62,66–81]. This gauge symmetry generates textures that produce flavor changes in the neutral currents and that, in principle, could be seen in future colliders. There are models with electroweak extensions of the SM such as $SO(14)$, $SU(9)$, 3-3-1, $U(1)_X$, etc. [82–97] that attempt to explain the flavor and the mass hierarchy problem of the SM. Another mechanism to generate textures in the Yukawa Lagrangian is through additional discrete or global symmetries. Some groups that have been used in the literature are: S_3, A_4, Δ_{27}, Z_2, etc. [98–110]. The simplest symmetries are of abelian type, which can be used to impose texture-zeros in the mass matrices to make them predictive. On the other hand, given fermion mass matrices with texture-zeros, it is possible to find an extended scalar sector so that the texture-zeros can be generated from abelian symmetries [58,59].

Due to the fact that there are three up-type quarks and three down-type quarks, the mass operators are 3×3 complex matrices with 36 degrees of freedom. If we consider these operators to be Hermitian [111–113], the number of free parameters reduces to 18, which cannot be fully determined from the 10 available physical quantities, namely masses and mixing angles [114]. This provides freedom to reduce the number of free parameters in the matrices and search for matrix structures with zeros that provide eigenvalues and mixing angles consistent with the masses and mixing matrices of the fermions. One way to find zeros in the mass matrices that is automatically consistent with experimental data is based on weak basis transformations (WBT) for quarks and leptons [112,113,115,116]. Fritzsch proposed an ansatz with six zeros [117,118,118–122], but the value of $|V_{ub}/V_{cb}| \approx 0.06$ is too small compared to the experimental value $|V_{ub}/V_{cb}|_{exp} \approx 0.09$ [123]. For this reason, the use of 4 and 5 zero-textures was proposed [111,112,122,124–127]. References [111,113] showed that matrices with five zero-textures could reproduce the mass hierarchy and mixing angles of the CKM matrix.

The strong CP problem arises from the fact that the QCD Lagrangian has a non-perturbative term ("θ-term") that explicitly violates CP in strong interactions. On the other hand, the possible connection between the strong CP problem and flavor problems was first mentioned in [128], and in later works [129–133]. Some recent studies and further references in the same direction are found in [59,129,134–146]. Peccei and Quinn proposed a solution to the strong CP problem [147,148], where it is assumed that the SM has an additional global chiral symmetry $U(1)$, which is spontaneously broken at a large energy scale f_a. One consequence of this breaking is the existence of a particle called the axion, which is the Goldstone boson of the broken $U(1)_{PQ}$ symmetry [149,150]. Due to the fact that the PQ symmetry is not exact at the quantum level, as a result of a chiral anomaly, the axion is massive and its mass (see Appendix D) is given by:

$$m_a = \frac{f_\pi m_\pi}{f_a}\frac{\sqrt{z}}{1+z} \approx 6\mu eV\left(\frac{10^{12}GeV}{f_a}\right), \tag{1}$$

where $z = 0.56$ is assumed for the up and down quark mass ratio, while $f_\pi \approx 92$ MeV and $m_\pi = 135$ MeV are the pion decay constant and mass, respectively.

The effective couplings of axions to ordinary particles are inversely proportional to f_a, and also depend on the model. It was originally thought that the PQ symmetry breaking occurred at the electroweak scale, but experiments have ruled this out. The mass of the axion and its coupling to matter and radiation scale as $1/f_a$, making its direct detection extremely difficult. The combined limits from unsuccessful searches in nuclear and particle physics experiments and from stellar evolution imply that $f_a \geq 3 \times 10^9$ GeV [151]. Furthermore, there is an upper limit of $f_a \leq 10^{12}$GeV that comes from cosmology, since light axions are produced in abundance during the QCD phase transition [152–156]. Hence, these models are generically referred to as "invisible" axion models and remain phenomenologically viable. There are two classes of invisible axion models in the literature: KSVZ (Kim, Shifman, Vainshtein, and Zakharov) [151,157] and DFSZ (Dine, Fischler, Srednicki, and Zhitnitsky) [158,159]. The main difference between KSVZ-type and DFSZ-type axions is that the former do not couple to ordinary quarks and leptons at tree level, but instead require an exotic quark that ensures a nonzero QCD anomaly to generate CP violation. Depending on the assumed value of f_a, the existence of axions could have interesting consequences in astrophysics and cosmology. The emission of axions produced in stellar plasma through their coupling to photons, electrons, and nucleons would provide a new mechanism for energy loss in stars. This could accelerate the evolutionary process of stars and, therefore, shorten their lifespan. Axions can also exist as primordial cosmic relics produced copiously in early times and could be candidates for dark matter. From numerous laboratory experiments and astrophysical observations, together with the cosmological requirement that the contribution to the mass density of the Universe from relic axions does not saturate the Universe. In post-inflationary scenarios, these constraints restrict the allowed values of the axion mass to a range of of [160] 10^{-5} eV $< m_a < 10^{-4}$ eV. One source of axions would be the Sun, which, coupled to two photons, could be produced through the Primakoff conversion of thermal photons in the electric and magnetic fields of the solar plasma. The limits are primarily useful for complementing the arguments of stellar energy loss [161] and the searches for solar axions by CAST at CERN [162] and the Tokyo axion helioscope [163].

The axion–photon coupling (see Appendix D) can be calculated in chiral perturbation theory as [147,148].

$$g_{a\gamma} = -\frac{\alpha}{2\pi f_a}\left(\frac{E}{N} - \frac{2}{3}\frac{z+4}{z+1}\right). \tag{2}$$

This coupling and the axion mass are related to each other through the relation E/N, which depends on the model and can be tested in experiments.

The strongest limits on the axion-electron coupling are derived from observations of stars with a dense core, where bremsstrahlung is very effective. These conditions are realized in White Dwarfs and Red Giant Stars, where the evolution of a White Dwarf is a cooling process by photon radiation and neutrino emission, with the possible addition of new energy loss channels such as axions. Current numerical analysis suggest a limit of $g_{ae} \leq 2.8 \times 10^{-13}$ [160]. In particular, using data from the Sloan Digital Sky Survey (SDSS) and SuperCOSMOS Sky Survey (SCSS) [164], they showed that the axion-electron coupling is approximately 1.4×10^{-13}. In a more recent analysis of the data in Ref. [164] by interpreting anomalous cooling observations in White Dwarfs and Red Giant Stars as a consequence of additional cooling channels induced by axions, the axion-electron coupling is determined to lie within the 2 σ confidence interval $g_{ae} = 1.5^{+0.6}_{-0.9} \times 10^{-13}$ (95% CL) [165,166]. The two groups studying the axion-electron coupling are M5 [161] and M3 [167]. Their combination yields the limit $g_{ae} = 1.6^{+0.29}_{-0.34} \times 10^{-13}$. For a recent and comprehensive review of axion physics, see [160].

This document is organized as follows: In Sect. 2, we review the textures for the quark and lepton mass matrices that will be used in this work. We also write the real parameters of these matrices in terms of the masses of the SM fermions and two free parameters. In Sect. 3, we present the particle content of our model and the necessary PQ charges to generate the mass matrix textures presented in Sect. 2. In Sect. 4, we adjust the Yukawa couplings to obtain the masses of the charged leptons and neutrinos. It is important to note that we cannot use the VEVs to adjust the lepton masses, as these were already adjusted to reproduce the quark masses. It is also important to note that by using a seesaw mechanism, we can avoid adjusting the Yukawas, however, that is not our purpose in the present work. In Sect. 5, we show the Lagrangian of our model. In Sect. 6, we present some constraints in the parameter space, as well as projected constraints for upcoming experimental results, both for experiments under construction and in the data-taking phase.

2 The five texture-zero mass matrices

The reason for dealing with texture zeros in the Standard Model (SM) and its extensions is to simplify as much as possible the number of free parameters that allow us to see relationships between masses and mixings present in these models. The Yukawa Lagrangian is responsible for giving mass to SM fermions after spontaneous symmetry breaking. A first simplification, without losing generality, is to consider that the fermion mass matrices are Hermitian, so the number of free parameters for each sector of quarks and leptons is reduced to 18, but there is still an excess of parameters to reproduce the experimental data provided in the literature. Due to the lack of a model to make predictions, discrete symmetries can be used to prohibit some components in the

Yukawa matrix, generating the so-called texture zeros for the mass matrices. In many works, instead of proposing discrete symmetries, texture zeros are proposed as practical and direct alternatives. The advantage of this approach is that it is possible to choose each mass matrix in an optimal way for the analytical treatment of the problem, and at the same time adjust the mixing angles and the masses of the fermions.

2.1 Quark sector

We should keep in mind that six-zero textures in the SM have already been discarded because their predictions are outside the experimental ranges allowed; but, five-zero textures for quark mass matrices is a viable possibility [55,115,168–171]. Specifically, we chose the following five-zero textures because they fit well with experimental quark masses and mixing parameters [111,113,172]:

$$M^U = \begin{pmatrix} 0 & 0 & C_u \\ 0 & A_u & B_u \\ C_u^* & B_u^* & D_u \end{pmatrix}, \qquad M^D = \begin{pmatrix} 0 & C_d & 0 \\ C_d^* & 0 & B_d \\ 0 & B_d^* & A_d \end{pmatrix}. \tag{3}$$

In addition, the phases in M^D can be removed by a weak basis transformation (WBT) [111,112,116], so that they are absorbed by the off-diagonal terms in M^U. In this way, the mass matrices (3) can be rewritten as:

$$M^U = \begin{pmatrix} 0 & 0 & |C_u|e^{i\phi_{C_u}} \\ 0 & A_u & |B_u|e^{i\phi_{B_u}} \\ |C_u|e^{-i\phi_{C_u}} & |B_u|e^{-i\phi_{B_u}} & D_u \end{pmatrix}, \qquad M^D = \begin{pmatrix} 0 & |C_d| & 0 \\ |C_d| & 0 & |B_d| \\ 0 & |B_d| & A_d \end{pmatrix}, \tag{4}$$

By applying the trace and the determinant to the mass matrices (4), before and after the diagonalization process, the free real parameters of M^U and M^D can be written in terms of their masses:

$$D_u = m_u - m_c + m_t - A_u, \tag{5a}$$

$$|B_u| = \sqrt{\frac{(A_u - m_u)(A_u + m_c)(m_t - A_u)}{A_u}}, \tag{5b}$$

$$|C_u| = \sqrt{\frac{m_u\, m_c\, m_t}{A_u}}, \tag{5c}$$

$$A_d = m_d - m_s + m_b, \tag{5d}$$

$$|B_d| = \sqrt{\frac{(m_b - m_s)(m_d + m_b)(m_s - m_d)}{m_d - m_s + m_b}}, \tag{5e}$$

$$|C_d| = \sqrt{\frac{m_d\, m_s\, m_b}{m_d - m_s + m_b}}. \tag{5f}$$

A possibility that works very well is to consider the second generation of quark masses to be negative, i.e., with eigenvalues $-m_c$ and $-m_s$. And A_u is a free parameter, whose value, determined by the quark mass hierarchy, must be in the following range:

$$m_u \leq A_u \leq m_t. \tag{6}$$

The exact analytical procedure for diagonalizing the mass matrices (4) is indicated in Appendix C.

2.2 Lepton sector

In this work, we will consider Dirac neutrinos. This is achieved, in part, by extending the SM with right-handed neutrinos. In this way, we can carry out a treatment similar to that of the quark sector, that is, the mass matrices of the lepton sector can be considered Hermitian and the weak basis transformation (WBT) can be applied [111,112]. In the literature, work has been done considering various texture-zeros for the Dirac mass matrices of the lepton sector [53,173–184]. In our treatment, we are going to consider the following five-zero texture model studied in the paper [126], which can accurately reproduce the Pontecorvo–Maki–Nakagawa–Sakata (PMNS) mixing matrix V_{PMNS} (mixing angles and the CP violating phase), the charged lepton masses, and the squared mass differences in the normal mass ordering.

$$M^N = \begin{pmatrix} 0 & |C_\nu|e^{ic_\nu} & 0 \\ |C_\nu|e^{-ic_\nu} & E_\nu & |B_\nu|e^{ib_\nu} \\ 0 & |B_\nu|e^{-ib_\nu} & A_\nu \end{pmatrix}, \qquad M^E = \begin{pmatrix} 0 & |C_\ell| & 0 \\ |C_\ell| & 0 & |B_\ell| \\ 0 & |B_\ell| & A_\ell \end{pmatrix}. \tag{7}$$

Without loss of generality, by using a WBT, the phases of the charged lepton mass matrix, M^E, can be absorbed into the entries C_ν and B_ν of the neutrino mass matrix, M^N. Similarly, as was done in the case of the quark sector, the parameters present in the mass matrices of the lepton sector (7) can be expressed in terms of the masses of the charged leptons m_e, m_μ and m_τ and the masses of the neutrinos m_1, m_2 and m_3, in the normal ordering ($m_1 < m_2 < m_3$):

$$A_\ell = m_e - m_\mu + m_\tau, \tag{8a}$$

$$|B_\ell| = \sqrt{\frac{(m_\tau - m_\mu)(m_e + m_\tau)(m_\mu - m_e)}{m_e - m_\mu + m_\tau}}, \tag{8b}$$

$$|C_\ell| = \sqrt{\frac{m_e m_\mu m_\tau}{m_e - m_\mu + m_\tau}}, \tag{8c}$$

$$E_\nu = m_1 - m_2 + m_3 - A_\nu, \tag{8d}$$

$$|B_\nu| = \sqrt{\frac{(A_\nu - m_1)(A_\nu + m_2)(m_3 - A_\nu)}{A_\nu}}, \tag{8e}$$

$$|C_\nu| = \sqrt{\frac{m_1 m_2 m_3}{A_\nu}}, \tag{8f}$$

where the values of the masses and the parameter A_ν are given in Table 5. Furthermore, for the adjustment of the mass matrices (7) it is very convenient to assume that the eigenvalues associated with the masses of the second family, $-m_2$ and $-m_\mu$, are negative quantities. The exact diagonalizing matrices of the mass matrices (7) are shown in Appendix C, Eqs. (49), (50) and (51).

3 PQ symmetry and the minimal particle content

3.1 Yukawa Lagrangian and the PQ symmetry

The texture-zeros of the mass matrices defined in the Eqs. (4) and (7) can be generated by imposing a Peccei–Queen symmetry $U(1)_{PQ}$ on the Lagrangian model, Eq. (9) [59,185,186]. As will be explained below, the minimal Lagrangian that allows us to implement this symmetry is given by [58,187]

$$\begin{aligned}\mathcal{L}_{\rm LO} \supset\ & (D_\mu \Phi^\alpha)^\dagger D^\mu \Phi^\alpha + \sum_\psi i\bar{\psi}\gamma^\mu D_\mu \psi + \sum_{i=1}^{2}(D_\mu S_i)^\dagger D^\mu S_i \\ & - \Big(\bar{q}_{Li}\, y_{ij}^{D\alpha}\Phi^\alpha d_{Rj} + \bar{q}_{Li}\, y_{ij}^{U\alpha}\tilde{\Phi}^\alpha u_{Rj} \\ & + \bar{\ell}_{Li}\, y_{ij}^{E\alpha}\Phi^\alpha e_{Rj} + \bar{\ell}_{Li}\, y_{ij}^{N\alpha}\tilde{\Phi}^\alpha \nu_{Rj} + \text{h.c}\Big) \\ & + (\lambda_Q \bar{Q}_R Q_L S_2 + \text{h.c}) - V(\Phi, S_1, S_2)\,. \end{aligned} \tag{9}$$

As it was shown in Ref. [58], at least four Higgs doublets are required to generate the quark mass textures, therefore $\alpha = 1,2,3,4$. In (9) i, j are family indices (there is an implicit sum over repeated indices). The superscripts U, D, E, N refer to up-type quarks, down-type quarks, electron-like and neutrino-like fermions, respectively; and $D_\mu = \partial_\mu + i\Gamma_\mu$ is the covariant derivative in the SM. The scalar potential $V(\Phi, S_1, S_2)$ is shown in appendix A (for further details, see Ref. [58]). In Eq. (9) ψ stands for the SM fermion fields plus the heavy quark Q (see Tables 1 and 2). As it is shown in Table 2 the PQ charges of the heavy quark can be chosen in such a way that only the interaction with the scalar singlet S_2 is allowed. We assign $Q_{\rm PQ}$ charges for the left-handed quark doublets (q_L): x_{q_i}, right-handed up-type quark singlets (u_R): x_{u_i}, right-handed down-type quark singlets (d_R): x_{d_i}, left-handed lepton doublets (ℓ_L): x_{ℓ_i}, right-handed charged leptons (e_R): x_{e_i} and right-handed Dirac neutrinos (ν_R): x_{ν_i} for each family ($i = 1,2,3$). We follow a similar notation for the scalar doublets, x_{ϕ_α} ($\alpha = 1,2,3,4$), and the scalar singlets $x_{S_{1,2}}$.

In this work, the PQ charges assigned to the quark sector and the scalar sector, as well as the VEVs assigned to the scalar doublets, will be the same as those assigned in [58] (Tables 1 and 2), and we will adjust the PQ charges of the lepton sector to reproduce the texture-zeros given in Eq. (7). To forbid a given entry in the lepton mass matrices, the corresponding sum of PQ charges must be different from zero, so that we can obtain texture-zeros by imposing the following conditions:

$$M^N = \begin{pmatrix} 0 & x & 0 \\ x & x & x \\ 0 & x & x \end{pmatrix} \longrightarrow \begin{pmatrix} S_{11}^{N\alpha} \neq 0 & S_{12}^{N\alpha} = 0 & S_{13}^{N\alpha} \neq 0 \\ S_{21}^{N\alpha} = 0 & S_{22}^{N\alpha} = 0 & S_{23}^{N\alpha} = 0 \\ S_{31}^{N\alpha} \neq 0 & S_{32}^{N\alpha} = 0 & S_{33}^{N\alpha} = 0 \end{pmatrix}, \tag{10}$$

$$M^E = \begin{pmatrix} 0 & x & 0 \\ x & 0 & x \\ 0 & x & x \end{pmatrix} \longrightarrow \begin{pmatrix} S_{11}^{E\alpha} \neq 0 & S_{12}^{E\alpha} = 0 & S_{13}^{E\alpha} \neq 0 \\ S_{21}^{E\alpha} = 0 & S_{22}^{E\alpha} \neq 0 & S_{23}^{E\alpha} = 0 \\ S_{31}^{E\alpha} \neq 0 & S_{32}^{E\alpha} = 0 & S_{33}^{E\alpha} = 0 \end{pmatrix}, \tag{11}$$

where $S_{ij}^{N\alpha} = (-x_{\ell_i} + x_{\nu_j} - x_{\phi_\alpha})$ and $S_{ij}^{E\alpha} = (-x_{\ell_i} + x_{e_j} + x_{\phi_\alpha})$.

Since the PQ charges of the Higgs doublets ($\alpha = 1,2,3,4$) are already given, the possible solutions of (10) and (11) are strongly constrained. Table 1 provides a solution for the PQ charges of the lepton sector.

In our model we include two scalar singlets S_1 and S_2 that break the global symmetry $U(1)_{PQ}$. The QCD anomaly of the PQ charges is

$$N = 2\sum_i^3 x_{q_i} - \sum_i^3 x_{u_i} - \sum_i^3 x_{d_i} + A_Q\,, \tag{12}$$

where $A_Q = x_{QL} - x_{QR}$ is the contribution to the anomaly of the heavy quark Q, which is a singlet under the electroweak gauge group, with left (right) Peccei-Quinn charges $x_{QL,R}$, respectively. We can write the charges as a function of N (since N must be different from zero), such that

$$s_1 = \frac{N}{9}\hat{s}_1, \qquad s_2 = \frac{N}{9}\left(\epsilon + \hat{s}_1\right), \quad \text{with} \quad \epsilon = 1 - \frac{A_Q}{N}\,, \tag{13}$$

where $\hat{s}_1$ and ϵ are arbitrary real numbers. To solve the strong CP problem with $N \neq 0$ and simultaneously generate the texture-zeros in the mass matrices, it is necessary to maintain $\epsilon = \frac{9(s_2 - s_1)}{N} \neq 0$. With these definitions for Flavor-Changing Neutral Currents (FCNC) observables, the relevant parameters are $\hat{s}_1$ and ϵ. This parameterization is quite convenient (for those cases where the parameters α_q and α_ℓ are not relevant) because by fixing N and f_a, we can vary $\hat{s}_1$ and ϵ for a fixed $\Lambda_{\rm PQ} = f_a N$ in such a way that the parameter space naturally reduces to two dimensions.

Table 1 Particle content. The subindex $i = 1, 2, 3$ stand for the family number in the interaction basis. Columns 6–8 are the Peccei-Quinn charges, Q_{PQ}, for each family of quarks and leptons in the SM. s_1, s_2 and α are real parameters, with $s_1 \neq s_2$

Particles	Spin	$SU(3)_C$	$SU(2)_L$	$U(1)_Y$	$U_{\rm PQ}(i=1)$	$U_{\rm PQ}(i=2)$	$U_{\rm PQ}(i=3)$	$Q_{\rm PQ}$
q_{Li}	1/2	3	2	1/6	$-2s_1+2s_2+\alpha_q$	$-s_1+s_2+\alpha_q$	α_q	x_{q_i}
u_{Ri}	1/2	3	1	2/3	$s_1+\alpha_q$	$s_2+\alpha_q$	$-s_1+2s_2+\alpha_q$	x_{u_i}
d_{Ri}	1/2	3	1	$-1/3$	$2s_1-3s_2+\alpha_q$	$s_1-2s_2+\alpha_q$	$-s_2+\alpha_q$	x_{d_i}
ℓ_{Li}	1/2	1	2	$-1/2$	$-2s_1+2s_2+\alpha_\ell$	$-s_1+s_2+\alpha_\ell$	α_ℓ	x_{ℓ_i}
e_{Ri}	1/2	1	1	-1	$2s_1-3s_2+\alpha_\ell$	$s_1-2s_2+\alpha_\ell$	$-s_2+\alpha_\ell$	x_{e_i}
ν_{Ri}	1/2	1	1	0	$-4s_1+5s_2+\alpha_\ell$	$-s_1+2s_2+\alpha_\ell$	$s_2+\alpha_\ell$	x_{ν_i}

Table 2 Beyond the SM fields and their respective PQ charges. The parameters s_1, s_2 are reals, with $s_1 \neq s_2$ and $x_{Q_R} \neq x_{Q_L}$

Particles	Spin	$SU(3)_C$	$SU(2)_L$	$U(1)_Y$	$U_{\rm PQ}$	$Q_{\rm PQ}$
Φ_1	0	1	2	1/2	s_1	x_{ϕ_1}
Φ_2	0	1	2	1/2	s_2	x_{ϕ_2}
Φ_3	0	1	2	1/2	$-s_1+2s_2$	x_{ϕ_3}
Φ_4	0	1	2	1/2	$-3s_1+4s_2$	x_{ϕ_4}
Q_L	1/2	3	1	0	x_{Q_L}	x_{Q_L}
Q_R	1/2	3	1	0	x_{Q_R}	x_{Q_R}
S_1	0	1	1	0	s_1-s_2	x_{s_1}
S_2	0	1	1	0	$x_{Q_R}-x_{Q_L}$	x_{s_2}

4 Naturalness of Yukawa couplings

4.1 The mass matrices in the quark sector

In Ref. [58], it was shown that to generate five texture zeros in the quark mass matrices (3), as a consequence of a PQ symmetry, it is necessary to include at least four scalar doublets in the model. After spontaneous symmetry breaking, the quark sector mass matrices take on the following form:

$$M^U = \hat{v}_\alpha y_{ij}^{U\alpha} = \begin{pmatrix} 0 & 0 & y_{13}^{U1}\hat{v}_1 \\ 0 & y_{22}^{U1}\hat{v}_1 & y_{23}^{U2}\hat{v}_2 \\ y_{13}^{U1*}\hat{v}_1 & y_{23}^{U2*}\hat{v}_2 & y_{33}^{U3}\hat{v}_3 \end{pmatrix},$$
$$M^D = \hat{v}_\alpha y_{ij}^{D\alpha} = \begin{pmatrix} 0 & |y_{12}^{D4}|\hat{v}_4 & 0 \\ |y_{12}^{D4}|\hat{v}_4 & 0 & |y_{23}^{D3}|\hat{v}_3 \\ 0 & |y_{23}^{D3}|\hat{v}_3 & y_{33}^{D2}\hat{v}_2 \end{pmatrix}, \quad (14)$$

where the $\hat{v}_i$ are defined in terms of the vacuum expectation values, $\hat{v}_i = v_i/\sqrt{2}$. In [58] it was shown that the five-texture zeros (4) are flexible enough to set the quark Yukawa couplings close to 1 for most of them (except for y_{23}^{U2}, y_{23}^{D3} and y_{13}^{U1}), in this way we obtain:

$$\hat{v}_1 = 1.71\,\text{GeV}, \qquad \hat{v}_2 = 2.91\,\text{GeV},$$
$$\hat{v}_3 = 174.085\,\text{GeV}, \qquad \hat{v}_4 = 13.3\,\text{MeV}. \quad (15)$$

As we can see, the hermiticity of the mass matrices is not fully achieved, but it is good to impose it for several reasons: (i) In the SM and its extensions, in which the right chirality fields are singlets under $SU(2)$, the mass matrices can be assumed Hermitian without losing generality, (ii) the previous fact allows us to consider Hermitian mass matrices, even after imposing an additional PQ symmetry in the model, (iii) we can implement the WBT method [111], and (iv) there is an extensive literature on physically viable Hermitian mass matrices. It is important to noticing that the mass matrices in Eq. (14) are Hermitian.

4.2 The mass matrices in the lepton sector

We can obtain the lepton mass matrices by starting from the Yukawa Lagrangian (9), which is invariant under the Peccei-Quinn $U(1)_{PQ}$ symmetry, and taking into account the Yukawa parameters and expectation values (15). After the spontaneous symmetry breaking, the mass matrices for neutral and charged leptons are given respectively by [126,188]:

$$M^N = \hat{v}_\alpha y_{ij}^{N\alpha} = \begin{pmatrix} 0 & y_{12}^{N1}\hat{v}_1 & 0 \\ y_{21}^{N4}\hat{v}_4 & y_{22}^{N2}\hat{v}_2 & y_{23}^{N1}\hat{v}_1 \\ 0 & y_{32}^{N3}\hat{v}_3 & y_{33}^{N2}\hat{v}_2 \end{pmatrix}, \quad (16)$$
$$M^E = \hat{v}_\alpha y_{ij}^{E\alpha} = \begin{pmatrix} 0 & |y_{12}^{E4}|\hat{v}_4 & 0 \\ |y_{12}^{E4}|\hat{v}_4 & 0 & |y_{23}^{E3}|\hat{v}_3 \\ 0 & |y_{23}^{E3}|\hat{v}_3 & y_{33}^{E2}\hat{v}_2 \end{pmatrix}. \quad (17)$$

As we previously mentioned, at least four Higgs doublets are needed to obtain the five texture-zeros for the chosen quark

mass matrices. Our goal in this work is to keep the same number of Higgs doublets and their respective PQ charges to generate the mass matrices and texture zeros for the lepton sector, Eq. (7). To get an Hermitian mass matrix M^N, it is necessary to impose $y_{21}^{N4}/y_{12}^{N1*} = \hat{v}_1/\hat{v}_4$ and $y_{32}^{N3}/y_{23}^{N1*} = \hat{v}_1/\hat{v}_3$, requiring that the diagonal elements be real, i.e., $y_{22}^{N2} = y_{22}^{N2*}$ and $y_{33}^{N2} = y_{33}^{N2*}$. On the other hand, to obtain a symmetric mass matrix, M^E, for the charged leptons, it is sufficient to assume that the Yukawa couplings are Hermitian. Through these choices it is possible to avoid additional Higgs doublets.

Based on the results of Table 5, Appendix C, and the relationships established in (8), we find the following values for the Yukawa couplings of the lepton sector:

$$
\begin{aligned}
|y_{12}^{E4}| &= 0.569582, & |y_{23}^{E3}| &= 0.00248291,\\
y_{33}^{E2} &= 0.574472, & |y_{12}^{N1}| &= 4.74362 \times 10^{-6},\\
|y_{21}^{N4}| &= 0.000609894, & y_{22}^{N2} &= 6.68808 \times 10^{-6},\\
|y_{23}^{N1}| &= 0.0000159881, & |y_{32}^{N3}| &= 1.57047 \times 10^{-7},\\
y_{33}^{N2} &= 8.65364 \times 10^{-6}.
\end{aligned}
$$

To reproduce the neutrino masses quoted in [126], in the SM is required a Yukawa coupling around 10^{-14}. In our case, the smallest Yukawa coupling is 10^{-7}, which significantly reduces the fine-tuning in comparison to that given by the SM.

5 The effective Lagrangian

The strongest constraints on non-universal PQ charges come from the FCNC. To determine these constraints, we start by writing the most general next-to-leading order (NLO) effective Lagrangian as [189,190]:

$$
\mathcal{L}_{\rm NLO} = c_{a\Phi^\alpha} O_{a\Phi^\alpha} + c_1 \frac{\alpha_1}{8\pi} O_B + c_2 \frac{\alpha_2}{8\pi} O_W + c_3 \frac{\alpha_3}{8\pi} O_G, \tag{18}
$$

$c_{a\Phi^\alpha}$ and $c_{1,2,3}$ are Wilson coefficients; $\alpha_{1,2,3} = \frac{g_{1,2,3}^2}{4\pi}$, where $g_{1,2,3}$ are the coupling strengths of the electroweak and strong interactions in the interaction basis; and the Wilson operators are:

$$
\begin{aligned}
O_{a\Phi} &= i \frac{\partial^\mu a}{\Lambda_{\rm PQ}} \left((D_\mu \Phi^\alpha)^\dagger \Phi^\alpha - \Phi^{\alpha\dagger} (D_\mu \Phi^\alpha) \right),\\
O_B &= -\frac{a}{\Lambda_{\rm PQ}} B_{\mu\nu} \tilde{B}^{\mu\nu},\\
O_W &= -\frac{a}{\Lambda_{\rm PQ}} W_{\mu\nu}^a \tilde{W}^{a\mu\nu},\\
O_G &= -\frac{a}{\Lambda_{\rm PQ}} G_{\mu\nu}^a \tilde{G}^{a\mu\nu},
\end{aligned} \tag{19}
$$

where B, W^a and G^a correspond to the gauge fields associated with the SM gauge groups $U(1)_Y$, $SU(2)_L$ and $SU(3)_C$, respectively. a is the axion field which corresponds to the CP odd component of S_1. It is possible to redefine the fields by multiplying by a phase

$$
\begin{aligned}
\Phi^\alpha &\longrightarrow e^{i \frac{x_{\Phi^\alpha}}{\Lambda_{\rm PQ}} a} \Phi^\alpha,\\
\psi_L &\longrightarrow e^{i \frac{x_{\psi_L}}{\Lambda_{\rm PQ}} a} \psi_L,\\
\psi_R &\longrightarrow e^{i \frac{x_{\psi_R}}{\Lambda_{\rm PQ}} a} \psi_R,\\
S_i &\longrightarrow e^{i \frac{x_{S_i}}{\Lambda_{\rm PQ}} a} S_i.
\end{aligned} \tag{20}
$$

In this expression, x_ψ corresponds to the PQ charges of the SM fermions, i.e., $\{x_{\psi_{L,R}}\} = \{x_{q_i}, x_{u_i}, x_{d_i}, x_{l_i}, x_{e_i}, x_{\nu_i}\}$ and $\{x_{\Phi^\alpha}\}$ are the PQ charges of the Higgs doublets $\{\Phi^\alpha\}$. Replacing these definitions in the kinetic terms of Eq. (9), we obtain new contributions to the effective Lagrangian Eq. (18) (the NLO contributions in the non-derivative terms cancel out). The leading order (LO) terms in $\Lambda_{\rm PQ}^{-1}$ can be written as [187,189]:

$$
\mathcal{L}_{\rm NLO} \longrightarrow \mathcal{L}_{\rm NLO} + \Delta\mathcal{L}_{\rm NLO}, \tag{21}
$$

where

$$
\Delta\mathcal{L}_{\rm NLO} = \Delta\mathcal{L}_{K^\Phi} + \Delta\mathcal{L}_{K^\psi} + \Delta\mathcal{L}_{K^S} + \Delta\mathcal{L}(F_{\mu\nu}), \tag{22}
$$

with

$$
\begin{aligned}
\Delta\mathcal{L}_{K^\Phi} &= i x_{\Phi^\alpha} \frac{\partial^\mu a}{\Lambda_{\rm PQ}} \left[(D_\mu \Phi^\alpha)^\dagger \Phi^\alpha - \Phi^{\alpha\dagger} (D_\mu \Phi^\alpha) \right],\\
\Delta\mathcal{L}_{K^\psi} &= \frac{\partial_\mu a}{2\Lambda_{\rm PQ}} \sum_\psi (x_{\psi_L} - x_{\psi_R}) \bar{\psi} \gamma^\mu \gamma^5 \psi\\
&\quad - (x_{\psi_L} + x_{\psi_R}) \bar{\psi} \gamma^\mu \psi,\\
\Delta\mathcal{L}_{K^S} &= i x_{S_i} \frac{\partial^\mu a}{\Lambda_{\rm PQ}} \left[(D_\mu S_i)^\dagger S_i - S_i^\dagger (D_\mu S_i) \right] + \text{h.c}\,.
\end{aligned} \tag{23}
$$

The field redefinitions (20) induce a modification in the measure of the functional path integral whose effects can be obtained from the divergence of the axial-vector current: $J_\mu^{PQ5} = \sum_\psi (x_{\psi_L} - x_{\psi_R}) \bar{\psi} \gamma_\mu \gamma^5 \psi$ [191],

$$
\begin{aligned}
\partial^\mu J_\mu^{PQ5} &= \sum_\psi 2 i m_\psi (x_{\psi_L} - x_{\psi_R}) \bar{\psi} \gamma^5 \psi\\
&\quad - \sum_\psi (x_{\psi_L} - x_{\psi_R}) \frac{\alpha_1 Y^2(\psi)}{2\pi} B_{\mu\nu} \tilde{B}^{\mu\nu}
\end{aligned}
$$

$$- \sum_{SU(2)_L \text{doublets}} x_{\psi_L} \frac{\alpha_2}{4\pi} W^a_{\mu\nu} \tilde{W}^{a\mu\nu} - \sum_{SU(3)\text{triplets}} (x_{\psi_L} - x_{\psi_R}) \frac{\alpha_3}{4\pi} G^a_{\mu\nu} \tilde{G}^{a\mu\nu}, \tag{24}$$

where the hypercharge is normalized by $Q = T_{3L} + Y$. The relation (24) is an on-shell relation, which is consistent with the momentum of an on-shell axion.

Substituting this result into $\mathcal{L}_{K^\psi} = \frac{\partial^\mu a}{2\Lambda_{\rm PQ}} J^{PQ5}_\mu = -\frac{a}{2\Lambda_{\rm PQ}} \partial^\mu J^{PQ5}_\mu$ we obtain new contributions to the leading-order Wilson coefficients [192]

$$\begin{aligned} c_1 &\longrightarrow c_1 - \frac{1}{3}\Sigma q + \frac{8}{3}\Sigma u + \frac{2}{3}\Sigma d - \Sigma \ell + 2\Sigma e, \\ c_2 &\longrightarrow c_2 - 3\Sigma q - \Sigma \ell, \\ c_3 &\longrightarrow c_3 - 2\Sigma q + \Sigma u + \Sigma d - A_Q, \end{aligned} \tag{25}$$

where $\Sigma q \equiv x_{q_1} + x_{q_2} + x_{q_3}$. The corresponding NLO Lagrangian is

$$\begin{aligned} \Delta\mathcal{L}(F_{\mu\nu}) = &\frac{a}{\Lambda_{\rm PQ}} \frac{\alpha_1}{8\pi} B_{\mu\nu} \tilde{B}^{\mu\nu} \left(\frac{1}{3}\Sigma q - \frac{8}{3}\Sigma u - \frac{2}{3}\Sigma d + \Sigma \ell - 2\Sigma e \right) \\ &+ \frac{a}{\Lambda_{\rm PQ}} \frac{\alpha_2}{8\pi} W^a_{\mu\nu} \tilde{W}^{a\mu\nu} \left(3\Sigma q + \Sigma \ell\right) \\ &+ \frac{a}{\Lambda_{\rm PQ}} \frac{\alpha_3}{8\pi} G^a_{\mu\nu} \tilde{G}^{a\mu\nu} \left(2\Sigma q - \Sigma u - \Sigma d + A_Q\right). \end{aligned} \tag{26}$$

It is convenient to define $c_3^{\rm eff} = c_3 - 2\Sigma q + \Sigma u + \Sigma d - A_Q = -N$. In our case, $c_i = 0$ and the only contributions to $c_i^{\rm eff}$ come from the anomaly. It is customary to define $\Lambda_{\rm PQ} = f_a |c_3^{\rm eff}|$ to include the factor $c_3^{\rm eff}$ in the normalization of the PQ charges. From now on, we will assume that all the PQ charges are normalized in this way, so that x_ψ corresponds to $x_\psi / c_3^{\rm eff}$. For normalized charges, $c_3^{\rm eff} = 1$, therefore, we still maintain the general form despite writing all the expressions in terms of the effective scale f_a.

The scalar fields and their PQ charges are the same as in the Ref. [58], so the scalar potential $V(\Phi, S)$ is identical to that of the mentioned reference. With the VEVs and couplings given in [58], the model reproduces the mass of the SM Higgs, while the masses of the exotic scalars are above the TeV scale. This potential has the appropriate number of Goldstone bosons to give masses to the SM gauge bosons Z^0, $W^\pm$ and has an extra field that can be identified with the axion a.

6 Low energy constraints

6.1 Flavor changing neutral currents

Due to the non-universal PQ charges in our model, a tree-level analysis of flavor-changing neutral currents is necessary. As mentioned in Ref. [160], the strongest limits on the axion-quark FCNC couplings come from meson decays in light mesons and missing energy.

The decays $K^\pm \to \pi^\pm a$ provide the tightest limits (NA62 Collaboration [193]) for the axion mass [160]. Currently the most restrictive limits come from the semileptonic decays of kaons $K^\pm \to \pi^\pm \bar{\nu}\nu$ and leptons $\ell_1 \to \ell_2$+missing energy. From the term $\Delta\mathcal{L}_{K^\psi}$, we obtain the vector and axial couplings for a multi-Higgs sector model, as shown in Refs. [58,160]

$$\Delta\mathcal{L}_{K^\psi} = -\partial_\mu a \bar{f}_i \gamma^\mu \left(g^V_{af_if_j} + \gamma^5 g^A_{af_if_j} \right) f_j, \tag{27}$$

where

$$g^{V,A}_{af_if_j} = \frac{1}{2 f_a c_3^{\rm eff}} \Delta^{Fij}_{V,A}, \tag{28}$$

where:

$$\Delta^{Fij}_{V,A} = \Delta^{Fij}_{RR}(d) \pm \Delta^{Fij}_{LL}(q), \tag{29}$$

with $\Delta^{Fij}_{LL}(q) = \left(U^F_L x_q \, U^{F\dagger}_L \right)^{ij}$ and $\Delta^{Fij}_{RR}(d) = \left(U^F_R x_d \, U^{F\dagger}_R \right)^{ij}$. In these expressions, F stands for U, D, N or E and the $U^F_{L,R}$ are de diagonalizing matrices (see Appendix C). In Eq. (28), we normalize the charges using $c_3^{\rm eff}$, as explained in the last paragraph of Sect. 5 (in other references $|c_3^{\rm eff}| = |N|$ is considered, corresponding to the $SU(3) \times U(1)_{PQ}$ anomaly). The branching ratio for lepton decays $\ell_i \to \ell_j a$ is given by [134]

$$\text{Br}(\ell_1 \to \ell_2 a) = \frac{m^3_{\ell_1}}{16\pi \Gamma(\ell_1)} \left(1 - \frac{m^2_{\ell_2}}{m^2_{\ell_1}} \right)^3 |g_{a\ell_1\ell_2}|^2,$$

in this expression, the vector and axial couplings contribute in the same way

$$|g_{a\ell_1\ell_2}|^2 = |g^V_{a\ell_1\ell_2}|^2 + |g^A_{a\ell_1\ell_2}|^2.$$

where m is the mass of the leptons and $\Gamma(\ell_i)$ is the total decay width of the particle ℓ_j.

For the lepton decay $\ell_i \to \ell_j a \gamma$, we can relate this branching ratio to the branching ratio of the process without the photon in the final state, according to the expression:

$$\text{Br}(\ell_1 \to \ell_2 a \gamma) = \left(\frac{\alpha}{2\pi} \int dx \, dy f(x, y) \right) \text{Br}(\ell_1 \to \ell_2 a),$$

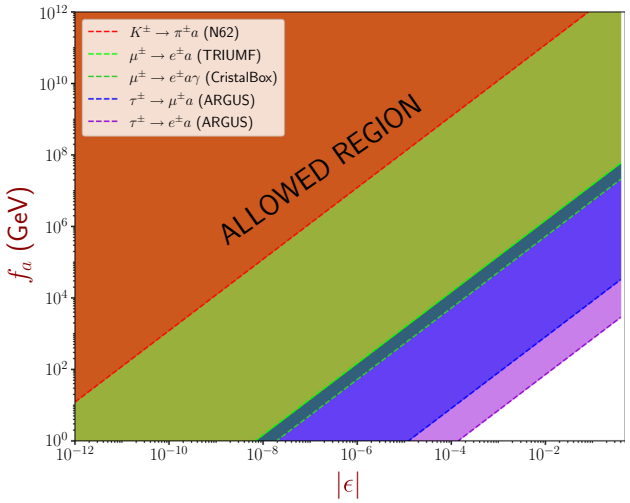

Fig. 1 Allowed regions by lepton decays. For the down-type quarks and charged leptons the non-universal part of the PQ charges just depend on the diference $s_2 - s_1 = N\epsilon/9$, hence the flavor-changing neutral-current couplings (the off diagonal elements) just depend on ϵ

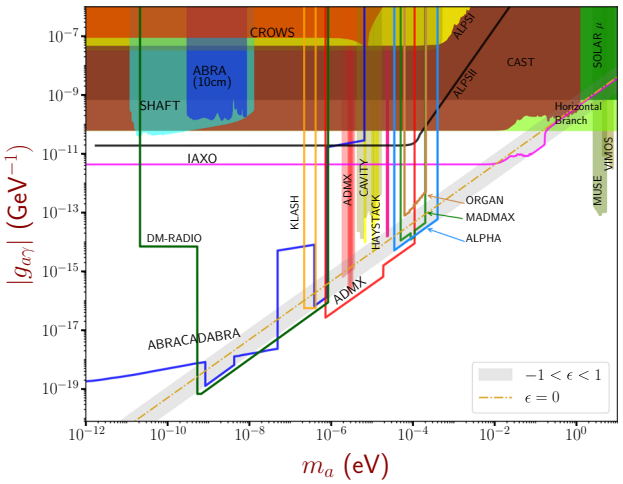

Fig. 2 The excluded parameter space by various experiments corresponds to the colored regions, the dashed-lines correspond to the projected bounds of coming experiments looking for axion signals [199]. The gray region corresponds to the parameter space scanned by our model

where α is the fine structure constant, and the function:

$$f(x, y) = \frac{(1-x)(2-y-xy)}{y^2(x+y-1)} \tag{30}$$

depends on the mass and the energies $x = 2E_{\ell_2}/m_{\ell_1}$ and $y = 2E_\gamma/m_{\ell_1}$. For the lepton decay $\mu \to e\,a\,\gamma$, the constraints come from the Crystal Box experiment [194], with cut energies $E_\gamma, E_e > 30\,\text{MeV}, \theta_{e\gamma} > 140°$, where:

$$\cos\theta_{e\gamma} = 1 + \frac{2(1-x-y)}{xy}, \tag{31}$$

so that $\int dx\,dy f(x, y) \approx 0.011$ (Table 3).

In our model, there is a natural alignment between the Φ_3 (which is quite similar to H_1 in the Georgi basis [198]) and the standard model Higgs boson as a consequence of the large suppression of the VEVs of the scalar doublets v_i, with $i = 1, 2, 4$, respect to v_3, the VEV of Φ_3. To some extent, this alignment avoids FCNC involving the SM Higgs boson [198]; however, after alignment, there are other sources of FCNC associated with the additional scalar doublets, which cannot be avoided by any means; however, as argued in Ref. [58] they are suppressed by a factor $1/M^4$ (where $M > 1\text{TeV}$ is the mass of the exotic scalar doublets), and therefore, our model avoids these potential sources of FCNC in agreement with the general argument presented in [198].

From astrophysical considerations we have: bounds from black holes superradiance and the SN 1987A upper limit on the neutron electric dipole moment, which, when combined, impose a constraint on the axion decay constant in the range [160] (see Fig. 1): $0.8 \times 10^6\text{GeV} \leq f_a \leq 2.8 \times 10^{17}\text{GeV}$.

6.2 Constraints on the axion–photon coupling

There are several experiments designed to look for exotic particles. The sources studied in the search for axions are: the solar axion flux (helioscopes experiments), dark matter halo (haloscopes experiments), and axions produced in the laboratory.

Among the experiments with the potential to search for evidence of axions in regions that cover areas within the limits established by the parameters of our model are: DM-Radio [200], KLASH [201,202], ADMX [203], ALPHA [204], MADMAX [205], IAXO [206,207] and ABRACADABRA [208]. Similarly, some experiments have already ruled out regions established by the parameters of our model, among which are: ADMX [209–211], CAST [212,213], CAPP [214–216], HAYSTACK [217,218], Solar ν [219], Horizontal Branch [220], MUSE [221] and VIMOS [222]

7 Discussion and conclusions

We have presented a model in which the fermion and scalar fields are charged under a $U(1)_{PQ}$ Peccei-Quinn symmetry. A recent work [58] showed that at least four Higgs doublets are required to generate Hermitian mass matrices in the quark sector with five texture-zeros, reproducing the quark masses, the mixing angles, and the CP-violating phase of the CKM mixing matrix. In this work, we show that using the same number of Higgs doublets, without changing the PQ charges in the quark and Higgs sectors, it is possible to generate Hermitian mass matrices in the lepton sector that reproduce the neutrino mass-squared differences in the normal mass

Table 3 These inequalities come from the window for new physics in the branching ratio uncertainty of the meson decay in a pair $\bar{\nu}\nu$

Collaboration	Upper bound
N62 collaboration [193]	$\mathcal{B}\left(K^+ \to \pi^+ a\right) < (10.6^{+4.0}_{-3.4}\big\vert_{stat} \pm 0.9_{syst}) \times 10^{-11}$
TRIUMF [195]	$\mathcal{B}\left(\mu^+ \to e^+ a\right) < 2.6 \times 10^{-6}$
Crystal Box [196]	$\mathcal{B}\left(\mu^+ \to e^+ \gamma a\right) < 1.1 \times 10^{-9}$
ARGUS [197]	$\mathcal{B}\left(\tau^+ \to e^+ a\right) < 1.5 \times 10^{-2}$
ARGUS [197]	$\mathcal{B}\left(\tau^+ \to \mu^+ a\right) < 2.6 \times 10^{-2}$

ordering, the mixing angles, and the CP-violating phase of the PMNS mixing matrix. This result is quite non-trivial as we maintain the same four Higgs doublets required in the quark sector to generate a different texture pattern in the lepton sector. When compared to the SM, our model has almost all Yukawa couplings close to 1 in the quark sector. In the neutrino sector, the smallest Yukawa coupling is of the order of 1.6×10^{-7}, which is seven orders of magnitude larger than the corresponding Yukawa coupling in the SM, so it requires less fine-tuning than the SM.

The polar decomposition theorem [223,224] allows any matrix to be written as the product of a Hermitian matrix and a unitary matrix. In the SM and in theories where the right-handed fermion fields are singlets under the gauge group, it is possible to absorb the unitary matrix into the right-handed fields by redefining them; from this procedure, we can write any mass matrix as a Hermitian matrix. In our work, we assume that the mass matrices are Hermitian in the interaction space, this hypothesis has been used in previous studies on textures [55,111,115,225–227], and it is quite useful for studying the flavor problem. In our work, we have normalized the PQ charges with the QCD anomaly $-N$ in such a way that by keeping the parameter $\epsilon \neq 0$, we obtain the textures of the mass matrices, addressing the flavor and strong CP problems simultaneously.

If nature is not fine-tuned in a more fundamental high-energy theory, we expect that, eventually, it will be possible to find a texture that allows us to obtain all the scales of the SM from the VEVs of a Higgs sector with a minimal scalar content without the need to adjust the Yukawa couplings.

In our analysis, we report the constraints from lepton decays and compare them with the constraints from the search for neutrino pairs in charged Kaon decays $K^{\pm} \longrightarrow \pi^{\pm}\bar{\nu}\nu$. The results are shown in Fig. 1, where the allowed region in the parameter space generated by ϵ and the axion decay constant f_a is displayed. This figure shows that the strongest constraints come from the semileptonic meson decay $K^{\pm} \to \pi\nu\bar{\nu}$. It is important to note that the lepton decays do not further constrain the parameter space of our model (compared to the region excluded by the meson decay). We also show the excluded regions for the axion–photon coupling as a function of the axion mass; these results are summarized in Fig. 2; the gray region corresponds to the parameter space of our model in the interval $-1 < \epsilon < 1$.

In this article, we have demonstrated that with four Higgs doublets, it is possible to fit the textures of the mass matrices, both in the lepton and quark sectors. These matrices generate the masses and the mixing matrices for quarks and leptons within the experimentally reported values in the literature. The introduction these doublets improves the fine-tuning problem of the Yukawa couplings and shows that this approach is a viable way to tackle the flavor problem. We hope to improve our results in future work by using the See-saw mechanism in the lepton sector.

Acknowledgements We thank Financial support from "Patrimonio Autónomo Fondo Nacional de Financiamiento para la Ciencia, la Tecnología y la Innovación, Francisco José de Caldas". This research was partly supported by the "Vicerrectoría de Investigaciones e Interacción Social VIIS de la Universidad de Nariño", project numbers 1928, 2172, 2686, 2693 and 2679. E.R and Y.G. acknowledge additional financial support from Minciencias CD 82315 CT ICETEX 2021-1080.

Data Availability Statement This manuscript has no associated data or the data will not be deposited. [Authors' comment: The article is self-contained, and that experimental data have been taken from published articles and correctly referenced].

Open Access This article is licensed under a Creative Commons Attribution 4.0 International License, which permits use, sharing, adaptation, distribution and reproduction in any medium or format, as long as you give appropriate credit to the original author(s) and the source, provide a link to the Creative Commons licence, and indicate if changes were made. The images or other third party material in this article are included in the article's Creative Commons licence, unless indicated otherwise in a credit line to the material. If material is not included in the article's Creative Commons licence and your intended use is not permitted by statutory regulation or exceeds the permitted use, you will need to obtain permission directly from the copyright holder. To view a copy of this licence, visit http://creativecommons.org/licenses/by/4.0/.
Funded by SCOAP^3. SCOAP^3 supports the goals of the International Year of Basic Sciences for Sustainable Development.

Appendix A: The mass operator matrices

The most general Yukawa Lagrangian for the interaction of four Higgs doublets Φ_α with the SM fermions is given by

$$\mathcal{L} = -\bar{q}'^i_L \Phi_\alpha y^{D\alpha}_{ij} d'^j_R - \bar{q}'^i_L \tilde{\Phi}_\alpha y^{U\alpha}_{ij} u'^j_R - \bar{\ell}'^i_L \Phi_\alpha y^{E\alpha}_{ij} e'^j_R$$

$$- \bar{\ell}_L'^i \tilde{\Phi}_\alpha y_{ij}^{N\alpha} \nu_R'^j + \text{h.c}, \tag{32}$$

where a sum is assumed on repeated indices. Here i, j run over $1, 2, 3$ and α over $1, 2, 3, 4$. The Higgs boson doublet fields are parameterized as follows:

$$\Phi_\alpha = \begin{pmatrix} \phi_\alpha^+ \\ \frac{v_\alpha + h_\alpha + i\eta_\alpha}{\sqrt{2}} \end{pmatrix}, \qquad \tilde{\Phi}_\alpha = i\sigma_2 \Phi_\alpha^*. \tag{33}$$

Similar to the two Higgs doublet model [228] we rotate the Higgs fields to the (generalized) Georgi basis, that is,

$$\begin{pmatrix} H_1 \\ H_2 \\ H_3 \\ H_4 \end{pmatrix} = R_1(\beta_1) R_2(\beta_2) R_3(\beta_3) \begin{pmatrix} \Phi_1 \\ \Phi_2 \\ \Phi_3 \\ \Phi_4 \end{pmatrix} \equiv R_{\beta\alpha} \Phi_\alpha, \tag{34}$$

where the orthogonal matrices

$$R_1(\beta_1) = \begin{pmatrix} \cos\beta_1 & \sin\beta_1 & 0 & 0 \\ -\sin\beta_1 & \cos\beta_1 & 0 & 0 \\ 0 & 0 & 1 & 0 \\ 0 & 0 & 0 & 1 \end{pmatrix}, \tag{35a}$$

$$R_2(\beta_2) = \begin{pmatrix} 1 & 0 & 0 & 0 \\ 0 & \cos\beta_2 & \sin\beta_2 & 0 \\ 0 & -\sin\beta_2 & \cos\beta_2 & 0 \\ 0 & 0 & 0 & 1 \end{pmatrix}, \tag{35b}$$

$$R_3(\beta_3) = \begin{pmatrix} 1 & 0 & 0 & 0 \\ 0 & 1 & 0 & 0 \\ 0 & 0 & \cos\beta_3 & \sin\beta_3 \\ 0 & 0 & -\sin\beta_3 & \cos\beta_3 \end{pmatrix}, \tag{35c}$$

where $\tan\beta_1 = \frac{\sqrt{v_2^2+v_3^2+v_4^2}}{v_1}$, $\tan\beta_2 = \frac{\sqrt{v_3^2+v_4^2}}{v_2}$ and $\tan\beta_3 = \frac{v_4}{v_3}$, and $H_\beta = (H_\beta^+, (H_\beta^0 + i H_\beta^{\text{odd}})/\sqrt{2})^{\text{T}}$. This basis is chosen in such a way that only the neutral component of H_1 acquires a vacuum expectation value

$$\begin{aligned} &\langle H_1^0 \rangle = \sqrt{v_1^2 + v_2^2 + v_3^2 + v_4^2} \equiv v, \\ &\langle H_2^0 \rangle = 0, \quad \langle H_3^0 \rangle = 0, \quad \langle H_4^0 \rangle = 0. \end{aligned} \tag{36}$$

In this way $\Phi_\alpha y_{ij}^{F\alpha} = y_{ij}^{F\alpha} R_{\alpha\beta}^T R_{\beta\gamma} \Phi_\gamma = \mathcal{Y}_{ij}^{F\beta} H_\beta$, and $F = U, D, N, E$; where we have defined

$$\mathcal{Y}_{ij}^{F\beta} = R_{\beta\alpha} y_{ij}^{F\alpha}. \tag{37}$$

With these definitions, Eq. (32) becomes

$$\begin{aligned} \mathcal{L} = &- \bar{q}_L'^i H_\beta \mathcal{Y}_{ij}^{D\beta} d_R'^j - \bar{q}_L'^i \tilde{H}_\beta \mathcal{Y}_{ij}^{U\beta} u_R'^j - \bar{\ell}_L'^i H_\beta \mathcal{Y}_{ij}^{E\beta} e_R'^j \\ &- \bar{\ell}_L'^i \tilde{H}_\beta \mathcal{Y}_{ij}^{N\beta} \nu_R'^j + \text{h.c}. \end{aligned} \tag{38}$$

It is necessary to rotate to the fermion mass eigenstates, i.e.,

$$f_{L,R} = U_{L,R}^F f_{L,R}', \tag{39}$$

where the diagonalization matrices $U_{L,R}$ are defined below, in Appendix C. From the Lagrangian for the charged currents

$$\begin{aligned} \mathcal{L}_{CC} &= -\frac{g}{\sqrt{2}} \bar{u}_{Li}' \gamma^\mu d_{Li}' W^+ - \frac{g}{\sqrt{2}} \bar{e}_{Li}' \gamma^\mu \nu_{Li}' W^- + \text{h.c} \\ &= -\frac{g}{\sqrt{2}} \bar{u}_{Li} \gamma^\mu \left(V_{\text{CKM}}\right)_{ij} d_{Lj} W^+ \\ &\quad - \frac{g}{\sqrt{2}} \bar{e}_{Li} \gamma^\mu \left(V_{\text{PMNS}}\right)_{ij} \nu_{Lj} W^- + \text{h.c}, \end{aligned} \tag{40}$$

it is possible to obtain the CKM ($V_{\text{CKM}} = U_L^U U_L^{D\dagger}$) and PMNS ($V_{\text{PMNS}} = U_L^E U_L^{\nu\dagger}$) mixing matrices by rotating to the fermion mass eigenstates. In particular, we are interested in the coupling of the axial neutral current to the axion in the mass eigenstates.

$$\begin{aligned} \mathcal{L}_{H^0} &= -\frac{1}{\sqrt{2}} \bar{d}_L'^i H_\beta^0 \mathcal{Y}_{ij}^{D\beta} d_R'^j - \frac{1}{\sqrt{2}} \bar{u}_L'^i H_\beta^{0*} \mathcal{Y}_{ij}^{U\beta} u_R'^j \\ &\quad - \frac{1}{\sqrt{2}} \bar{e}_L'^i H_\beta^0 \mathcal{Y}_{ij}^{E\beta} e_R'^j - \frac{1}{\sqrt{2}} \bar{\nu}_L'^i H_\beta^{0*} \mathcal{Y}_{ij}^{N\beta} \nu_R'^j + \text{h.c}, \\ &= -\frac{1}{\sqrt{2}} \bar{d}_L^i H_\beta^0 Y_{ij}^{D\beta} d_R^j - \frac{1}{\sqrt{2}} \bar{u}_L^i H_\beta^{0*} Y_{ij}^{U\beta} u_R^j \\ &\quad - \frac{1}{\sqrt{2}} \bar{e}_L^i H_\beta^0 Y_{ij}^{E\beta} e_R^j - \frac{1}{\sqrt{2}} \bar{\nu}_L^i H_\beta^{0*} Y_{ij}^{N\beta} \nu_R^j + \text{h.c}, \end{aligned}$$

where $Y_{ij}^{F\beta} = \left(U_L^F \mathcal{Y}^{F\beta} U_R^{F\dagger}\right)_{ij}$. In these expressions the mass functions in the interaction basis are:

$$\begin{aligned} M_{ij}^D &= \frac{v}{\sqrt{2}} \mathcal{Y}_{ij}^{D1}, \qquad M_{ij}^U = \frac{v}{\sqrt{2}} \mathcal{Y}_{ij}^{U1}, \\ M_{ij}^E &= \frac{v}{\sqrt{2}} \mathcal{Y}_{ij}^{E1}, \qquad M_{ij}^N = \frac{v}{\sqrt{2}} \mathcal{Y}_{ij}^{N1}, \end{aligned} \tag{41}$$

where $v = \langle H_1^0 \rangle$ is the Higgs vacuum expectation value.

Appendix B: Scalar potential

As studied in [58], the scalar sector requires four scalar doublets ϕ^α to reproduce the mass textures of the fermion sector correctly, and two scalar singlets S_1 and S_2 that break the PQ symmetry while generating a phenomenologically viable scalar mass spectrum. The S_2 singlet also gives mass to the heavy quark. The most general potential allowed by the PQ symmetry according to the charges established in Table 2 is:

$$V(\Phi, S_i) = \sum_{i=1}^4 \mu_i^2 \Phi_i^\dagger \Phi_i + \sum_{k=1}^2 \mu_{S_k}^2 S_k^* S_k + \sum_{i=1}^4 \lambda_i \left(\Phi_i^\dagger \Phi_i\right)^2$$

$$
\begin{aligned}
&+\sum_{k=1}^{2}\lambda_{s_k}\left(S_k^* S_k\right)^2+\sum_{i=1}^{4}\sum_{k=1}^{2}\lambda_{is_k}\left(\Phi_i^\dagger\Phi_i\right)\left(S_k^* S_k\right)\\
&+\underbrace{\sum_{i,\,j\,=1}^{4}}_{i<j}\left(\lambda_{ij}\left(\Phi_i^\dagger\Phi_i\right)\left(\Phi_j^\dagger\Phi_j\right)+J_{ij}\left(\Phi_i^\dagger\Phi_j\right)\left(\Phi_j^\dagger\Phi_i\right)\right)\\
&+\lambda_{s_1s_2}\left(S_1^* S_1\right)\left(S_2^* S_2\right)\\
&+K_1\left(\left(\Phi_1^\dagger\Phi_2\right)\left(\Phi_3^\dagger\Phi_2\right)+h.c.\right)\\
&+K_2\left(\left(\Phi_3^\dagger\Phi_4\right)\left(\Phi_3^\dagger\Phi_1\right)+h.c.\right)\\
&+F_1\left(\left(\Phi_2^\dagger\Phi_3\right)S_1+h.c.\right)\\
&+F_2\left(\left(\Phi_1^\dagger\Phi_2\right)S_1+h.c.\right)\\
&+\frac{1}{2}\left(m_{\zeta_{S_2}}\right)^2_{\mathrm{SB}}\zeta_{S_2}^2+\frac{1}{2}\left(m_{\xi_{S_2}}\right)^2_{\mathrm{SB}}\xi_{S_2}^2. \qquad (42)
\end{aligned}
$$

where the terms proportional to F_i are allowed by the particular choice of PQ charges and these couplings F_i have units of mass. After spontaneous symmetry breaking (SSB), the four Higgs doublets acquire VEVs that give mass to all the SM particles. The scalar doublets and singlets are written as follows:

$$
\begin{aligned}
\Phi_\alpha &= \begin{pmatrix}\phi_\alpha^+\\ \frac{v_\alpha+h_\alpha+i\eta_\alpha}{\sqrt{2}}\end{pmatrix}, \qquad \tilde{\Phi}_\alpha = i\sigma_2\Phi_\alpha^*, \alpha=1,2,3,4,\\
S_i &= \frac{v_{S_i}+\xi_{S_i}+i\zeta_{S_i}}{\sqrt{2}}; \qquad i=1,2, \qquad (43)
\end{aligned}
$$

where the VEVs satisfy the following hierarchy: $v_4 \ll v_1, v_2 \ll v_3 \ll v_{S_1} \sim v_{S_2}$. The scalar singlets S_1 and S_2 break the PQ symmetry at the high energy scale given by $v_{s_1} \approx v_{s_2}$. The last two terms in Eq. (42) correspond to the soft-breaking masses of the imaginary and the real parts of S_2, which are generated at one loop in the Coleman-Weinberg potential from the interaction term $\lambda_Q S_2 \bar{Q}_R Q_L + \text{h.c.}$ Additionally, we choose numerical values for the parameters of the potential (42) in order to obtain a scalar sector mass spectrum consistent with the existing phenomenology. The values of these parameters are:

$$
\begin{aligned}
\lambda_1 &= \lambda_2=\lambda_4=\lambda_{s_1}=\lambda_{s_2}=\lambda_{s_1s_2}=1,\\
\lambda_3 &= 0.463\\
\lambda_{ij} &= 1 \text{ for any } i,\, j,\\
\lambda_{js_1} &= \lambda_{js_2}=1 \text{ for any } j,\\
J_{12} &= J_{13}=J_{23}=J_{24}=-1, \quad \text{otherwise } J_{ij}=1,\\
K_1 &= K_2=-1,\\
F_1 &= F_2=-1\text{GeV}. \qquad (44)
\end{aligned}
$$

In particular, the value of λ_3 adjusts the SM Higgs mass. The v_i are determined from the SM fermion masses and the quark mass matrix textures, Eq. (15). The VEV v_{s_1} remains a free parameter; however, this parameter is important for the axion physics due to the relationship [165],

$$
f_a = \frac{v_{s_1}}{2N}. \qquad (45)
$$

In our calculations we took $v_{s_1} \approx v_{s_2} \approx 10^6$GeV. It is important to emphasize that in our model, f_a can take arbitrary values; nevertheless, a small f_a restricts ϵ (Eq. 13) to values close to zero. Taking into account all these considerations, including Eq. (44), the scalar mass spetrum (in GeV) is:

$$
\begin{aligned}
\text{CP even} &= \{1.73\times10^6,\, 1.\times10^6,\, 6.54\times10^3,\, 1.97\times10^3,\\
&\quad 1.09\times10^3,\, 125\},\\
\text{CP odd} &= \{6.54\times10^3,\, 1.97\times10^3,\, 1.09\times10^3,\, 0,\, 0,\, m_{\zeta_{S_2}}\},\\
\text{Charged fields} &= \{6.54\times10^3,\, 1.97\times10^3,\, 1.11\times10^3,\, 0\}. \qquad (46)
\end{aligned}
$$

The mass spectrum of the scalar fields is above the TeVs scale, except for the SM Higgs, which is at 125 GeV. The pseudoscalar sector (CP odd fields) have two massless eigenstates, the axion field and the Goldstone boson which is absorbed by the longitudinal component of the SM Z boson. A similar result is obtained in the charged sector, where it is possible to identify the two Goldstone bosons required to give mass to the SM $W^\pm$ fields.

Appendix C: diagonalization matrices

To compare with physical quantities, it is necessary to rotate fields to the mass eigenstates, i.e., $f_{L,R} = U^F_{L,R} f'_{L,R}$, where the prime symbol stands for the interaction basis. In our formalism the quark mass matrices are Hermitian, so the right- and left-handed diagonalizing matrices are identical; additionally, we establish that the eigenvalues of the second family of quarks are negative in order to generate texture-zeros in some diagonal terms of the mass matrices, as indicated in [112]. This sign is taken into account by introducing the identity matrix written as $I_2 I_2 = 1$ with $I_2 = \text{diag}(1,-1,1)$, i.e.,

$$
\begin{aligned}
M^F_{ij} &= \left(U^{F\dagger}\lambda^F U^F\right)_{ij} = \left(U^{F\dagger}_L m^F U^F_R\right)_{ij}\\
&= \frac{v}{\sqrt{2}}\mathcal{Y}^{F1}_{ij} = \frac{v}{\sqrt{2}}R_{1\alpha}y^{F\alpha}_{ij}, \qquad (47)
\end{aligned}
$$

where $\mathcal{Y}^{F\beta}_{ij}$ and $R_{\alpha\beta}$ were defined in Appendix A, $\lambda^{U,D} = \text{diag}(m_{u,d}, -m_{c,s}, m_{t,b})$ and $m^{U,D} = \text{diag}(m_{u,d}, m_{c,s}, m_{t,b})$, with similar definitions in the lepton sector, i.e., $\lambda^{N,E} = \text{diag}(m_{1,e}, -m_{2,\mu}, m_{3,\tau})$, $m^{N,E} = \text{diag}(m_{1,e}, m_{2,\mu}, m_{3,\tau})$, and

$$
U^F_L = U^F, \quad U^F_R = I_2 U^F, \qquad (48)
$$

where the U^F diagonalization matrices are defined below. It is important to stress that the texture-zeros pattern in the

matrix $\mathcal{Y}^{F1}_{ij}$ are identical to those in the original Yukawa couplings $y^{F\alpha}_{ij}$, since the sum over α does not mix the i, j indices. In fact, according to Eqs. (14) and (17), $M^F = \frac{v_\alpha}{\sqrt{2}} y^{F\alpha}_{ij} = \frac{v}{\sqrt{2}} R_{1\alpha} y^{F\alpha}_{ij}$, therefore $R_{1\alpha} = \frac{v_\alpha}{v}$. The diagonalization matrices are:

$$U^{U\dagger} = \begin{pmatrix} e^{i(\phi_{C_u}+\theta_{1u})}\sqrt{\frac{m_c m_t (A_u-m_u)}{A_u(m_c+m_u)(m_t-m_u)}} & -e^{i(\phi_{C_u}+\theta_{2u})}\sqrt{\frac{(A_u+m_c)m_t m_u}{A_u(m_c+m_t)(m_c+m_u)}} & e^{i(\phi_{C_u}+\theta_{3u})}\sqrt{\frac{m_c(m_t-A_u)m_u}{A_u(m_c+m_t)(m_t-m_u)}} \\ -e^{i(\phi_{B_u}+\theta_{1u})}\sqrt{\frac{(A_u+m_c)(m_t-A_u)m_u}{A_u(m_c+m_u)(m_t-m_u)}} & -e^{i(\phi_{B_u}+\theta_{2u})}\sqrt{\frac{m_c(m_t-A_u)(A_u-m_u)}{A_u(m_c+m_t)(m_c+m_u)}} & e^{i(\phi_{B_u}+\theta_{3u})}\sqrt{\frac{(A_u+m_c)m_t(A_u-m_u)}{A_u(m_c+m_t)(m_t-m_u)}} \\ e^{i\theta_{1u}}\sqrt{\frac{m_u(A_u-m_u)}{(m_c+m_u)(m_t-m_u)}} & e^{i\theta_{2u}}\sqrt{\frac{m_c(A_u+m_c)}{(m_c+m_t)(m_c+m_u)}} & e^{i\theta_{3u}}\sqrt{\frac{m_t(m_t-A_u)}{(m_c+m_t)(m_t-m_u)}} \end{pmatrix}, \quad (49)$$

$$U^{D\dagger} = \begin{pmatrix} e^{i\theta_{1d}}\sqrt{\frac{m_b(m_b-m_s)m_s}{(m_b-m_d)(m_d+m_s)(m_b+m_d-m_s)}} & -e^{i\theta_{2d}}\sqrt{\frac{m_b(m_b+m_d)m_d}{(m_d+m_s)(m_b+m_d-m_s)(m_b+m_s)}} & \sqrt{\frac{m_d(m_s-m_d)m_s}{(m_b-m_d)(m_b+m_d-m_s)(m_b+m_s)}} \\ e^{i\theta_{1d}}\sqrt{\frac{m_d(m_b-m_s)}{(m_b-m_d)(m_d+m_s)}} & e^{i\theta_{2d}}\sqrt{\frac{(m_b+m_d)m_s}{(m_d+m_s)(m_b+m_s)}} & \sqrt{\frac{m_b(m_s-m_d)}{(m_b-m_d)(m_b+m_s)}} \\ -e^{i\theta_{1d}}\sqrt{\frac{m_d(m_b+m_d)(m_s-m_d)}{(m_b-m_d)(m_d+m_s)(m_b+m_d-m_s)}} & -e^{i\theta_{2d}}\sqrt{\frac{(m_b-m_s)m_s(m_s-m_d)}{(m_d+m_s)(m_b+m_d-m_s)(m_b+m_s)}} & \sqrt{\frac{m_b(m_b+m_d)(m_b-m_s)}{(m_b-m_d)(m_b+m_d-m_s)(m_b+m_s)}} \end{pmatrix}, \quad (50)$$

where θ_{1u}, θ_{2u}, θ_{3u}, θ_{1d} and θ_{2d} are arbitrary phases (a third phase for the diagonalization matrix (50) can be absorbed by the remaining phases) that are useful for conforming to the $V_{\rm CKM} = U^U_L\, U^{D\dagger}_L$ matrix convention. Taking as input the SM parameters at the Z pole, the best fit values are given in Table 4.

Similarly, in the lepton sector, the diagonalization matrices of the mass matrices (7) are:

$$U^{N\dagger} = \begin{pmatrix} e^{i(\theta_{1\nu}+c_\nu)}\sqrt{\frac{m_2 m_3 (A_\nu-m_1)}{A_\nu(m_2+m_1)(m_3-m_1)}} & -e^{i(\theta_{2\nu}+c_\nu)}\sqrt{\frac{m_1 m_3 (m_2+A_\nu)}{A_\nu(m_2+m_1)(m_3+m_2)}} & e^{i(\theta_{3\nu}+c_\nu)}\sqrt{\frac{m_1 m_2 (m_3-A_\nu)}{A_\nu(m_3-m_1)(m_3+m_2)}} \\ e^{i\theta_{1\nu}}\sqrt{\frac{m_1(A_\nu-m_1)}{(m_1+m_2)(m_3-m_1)}} & e^{i\theta_{2\nu}}\sqrt{\frac{m_2(A_\nu+m_2)}{(m_2+m_1)(m_3+m_2)}} & e^{i\theta_{3\nu}}\sqrt{\frac{m_3(m_3-A_\nu)}{(m_3-m_1)(m_3+m_2)}} \\ -e^{i(\theta_{1\nu}-b_\nu)}\sqrt{\frac{m_1(A_\nu+m_2)(m_3-A_\nu)}{A_\nu(m_1+m_2)(m_3-m_1)}} & -e^{i(\theta_{2\nu}-b_\nu)}\sqrt{\frac{m_2(A_\nu-m_1)(m_3-A_\nu)}{A_\nu(m_2+m_1)(m_3+m_2)}} & e^{i(\theta_{3\nu}-b_\nu)}\sqrt{\frac{m_3(A_\nu-m_1)(A_\nu+m_2)}{A_\nu(m_3-m_1)(m_3+m_2)}} \end{pmatrix},$$

$$U^{E\dagger} = \begin{pmatrix} e^{i\theta_{1\ell}}\sqrt{\frac{m_\mu m_\tau (m_\tau-m_\mu)}{(m_e-m_\mu+m_\tau)(m_\mu+m_e)(m_\tau-m_e)}} & -e^{i\theta_{2\ell}}\sqrt{\frac{m_e m_\tau (m_e+m_\tau)}{(m_e-m_\mu+m_\tau)(m_\mu+m_e)(m_\tau+m_\mu)}} & \sqrt{\frac{m_e m_\mu (m_\mu-m_e)}{(m_e-m_\mu+m_\tau)(m_\tau-m_e)(m_\tau+m_\mu)}} \\ e^{i\theta_{1\ell}}\sqrt{\frac{m_e(m_\tau-m_\mu)}{(m_\mu+m_e)(m_\tau-m_e)}} & e^{i\theta_{2\ell}}\sqrt{\frac{m_\mu(m_e+m_\tau)}{(m_\mu+m_e)(m_\tau+m_\mu)}} & \sqrt{\frac{m_\tau(m_\mu-m_e)}{(m_\tau-m_e)(m_\tau+m_\mu)}} \\ -e^{i\theta_{1\ell}}\sqrt{\frac{m_e(m_e+m_\tau)(m_\mu-m_e)}{(m_e-m_\mu+m_\tau)(m_\mu+m_e)(m_\tau-m_e)}} & -e^{i\theta_{2\ell}}\sqrt{\frac{m_\mu(m_\tau-m_\mu)(m_\mu-m_e)}{(m_e-m_\mu+m_\tau)(m_\mu+m_e)(m_\tau+m_\mu)}} & \sqrt{\frac{m_\tau(m_\tau-m_\mu)(m_e+m_\tau)}{(m_e-m_\mu+m_\tau)(m_\tau-m_e)(m_\tau+m_\mu)}} \end{pmatrix}, \quad (51)$$

where $\theta_{1\ell}$, $\theta_{2\ell}$, $\theta_{1\nu}$, $\theta_{2\nu}$, $\theta_{3\nu}$ are necessary phases in order to adjust to the established convention for the PMNS mixing matrix [229] [1]; and c_ν and b_ν are the phases of C_ν and B_ν in the neutral mass matrix M^N in Eq. (7). The best fit values for these quantities are shown in Table 5.

Appendix D: Axion decay into photons

In the SM, $B^\mu = \cos\theta_W A^\mu - \sin\theta_W Z^\mu$ and $W^{3\mu} = \sin\theta_W A^\mu + \cos\theta_W Z^\mu$, where A^μ and Z^μ are the SM fields for the photon and Z gauge bosons, replacing these expresions in Eq. (26) we obtain

$$\begin{aligned} \mathcal{L} \supset & -c_1^{\rm eff}\frac{\alpha_1}{8\pi}\frac{a}{\Lambda_{\rm PQ}} B_{\mu\nu}\tilde{B}^{\mu\nu} - c_2^{\rm eff}\frac{\alpha_2}{8\pi}\frac{a}{\Lambda_{\rm PQ}} W^3_{\mu\nu}\tilde{W}^{3\mu\nu} \\ & = -\frac{\alpha}{8\pi}(c_1^{\rm eff}+c_2^{\rm eff})\frac{a}{\Lambda_{\rm PQ}} F_{\mu\nu}\tilde{F}^{\mu\nu} \\ & - \frac{\alpha}{8\pi c_W^2 s_W^2}(s_W^4 c_1^{\rm eff} + c_W^4 c_2^{\rm eff})\frac{a}{f_a} Z_{\mu\nu}\tilde{Z}^{\mu\nu} \\ & - \frac{2\alpha}{8\pi c_W s_W}(c_W^2 c_2^{\rm eff} - c_W^2 c_1^{\rm eff})\frac{a}{\Lambda_{\rm PQ}} F_{\mu\nu}\tilde{Z}^{\mu\nu} \\ & = e^2 C_{\gamma\gamma}\frac{a}{\Lambda_{\rm PQ}} F_{\mu\nu}\tilde{F}^{\mu\nu} + \frac{e^2 C_{ZZ}}{c_W^2 s_W^2}\frac{a}{\Lambda_{\rm PQ}} Z_{\mu\nu}\tilde{Z}^{\mu\nu} \\ & + \frac{2e^2 C_{\gamma Z}}{c_W s_W}\frac{a}{\Lambda_{\rm PQ}} F_{\mu\nu}\tilde{Z}^{\mu\nu} \end{aligned} \quad (52)$$

$$c_1^{\rm eff} = c_1 - \frac{1}{3}\Sigma q + \frac{8}{3}\Sigma u + \frac{2}{3}\Sigma d - \Sigma l + 2\Sigma e \quad (53)$$

$$c_2^{\rm eff} = c_2 - 3\Sigma q - \Sigma l \quad (54)$$

where $\Sigma f \equiv f_1 + f_2 + f_3$ is the sum of the PQ charges of the three families. There are similar definitions for the interaction of the axion with the gluons

$$-c_3^{\rm eff}\frac{\alpha_3}{8\pi}\frac{a}{\Lambda_{\rm PQ}} G^a_{\mu\nu}\tilde{G}^{a\mu\nu} = g_s^2 C_{GG}\frac{a}{\Lambda_{\rm PQ}} G^a_{\mu\nu}\tilde{G}^{a\mu\nu}, \quad (55)$$

[1] NuFIT collaboration (http://www.nu-fit.org/?q=node/211) (with SK atmospheric data).

Table 4 Best-fit point of the mass matrix parameters with respect to experimental data for the masses and mixing angles of the quark sector at the Z pole

θ_{1u}	θ_{2u}	θ_{3u}	θ_{1d}	θ_{2d}	ϕ_{C_u}	ϕ_{B_u}
−2.84403	1.85606	−0.00461668	1.93013	−0.976639	−1.49697	0.301461
A_u	m_u	m_c	m_t	m_d	m_s	m_b
1690.29 MeV	1.2684 MeV	633.197 MeV	171268 MeV	3.14751 MeV	56.1169 MeV	2910.01 MeV

Table 5 Best fit values

$\theta_{1\ell}$	$\theta_{2\ell}$	$\theta_{1\nu}$	$\theta_{2\nu}$	$\theta_{3\nu}$	c_ν	b_ν
0.154895	2.01797	−0.835504	2.21169	1.81786	1.01608	2.03726
A_ν (eV)	m_e (MeV)	m_μ (MeV)	m_τ (MeV)	m_1 (eV)	m_2 (eV)	m_3 (eV)
0.0251821	0.5109989461	105.6583745	1776.86	0.00353647	0.00929552	0.0504034

where $c_3^{\text{eff}} = c_3 - 2\Sigma q + \Sigma u + \Sigma d - A_Q$, in our particular case $c_i = 0$. In axion phenomenology, it is usual to define

$$C_{\gamma\gamma}=-\frac{1}{32\pi^2}(c_1^{\text{eff}}+c_2^{\text{eff}}),\ C_{ZZ}=-\frac{1}{32\pi^2}(s_W^4 c_1^{\text{eff}}+c_W^4 c_2^{\text{eff}}),$$
$$C_{\gamma Z}=-\frac{1}{32\pi^2}(c_W^2 c_2^{\text{eff}}-c_W^2 c_1^{\text{eff}}),\quad C_{GG}=-\frac{1}{32\pi^2}c_3^{\text{eff}}. \tag{56}$$

The decay widths of an axion decaying in two photons and a Z decaying in an axion and a photon are [191]

$$\Gamma(a\to\gamma\gamma)=\frac{4\pi\alpha^2 m_a^3}{\Lambda_{\text{PQ}}^2}|C_{\gamma\gamma}^{\text{eff}}|^2,$$
$$\Gamma(Z\to\gamma a)=\frac{8\pi\alpha(m_Z)m_Z^3}{3s_W^2c_W^2\Lambda_{\text{PQ}}^2}|C_{\gamma Z}^{\text{eff}}|^2\left(1-\frac{m_a^2}{m_Z^2}\right)^3. \tag{57}$$

Another possible decay channel of the axion in two photons is due to the mixing between the axion and the pion since the latter can decay in two photons, this decay mode generates an additional correction that only depends on the couplings of the axion to the gluons [230]

$$C_{\gamma\gamma}^{\text{eff}}=-\frac{c_3^{\text{eff}}}{32\pi^2}\left(\frac{c_1^{\text{eff}}+c_2^{\text{eff}}}{c_3^{\text{eff}}}-2.03\right),$$
$$C_{\gamma Z}^{\text{eff}}=-\frac{c_3^{\text{eff}}}{32\pi^2}\left(\frac{c_W^2c_2^{\text{eff}}-c_W^2c_1^{\text{eff}}}{c_3^{\text{eff}}}-0.74/2\right). \tag{58}$$

It is usual to define $\Lambda_{\text{PQ}} = |c_3^{\text{eff}}| f_a$.

$$\frac{E}{N}=\frac{c_1^{\text{eff}}+c_2^{\text{eff}}}{c_3^{\text{eff}}}. \tag{59}$$

The axion–photon interaction is given by

$$g_{a\gamma\gamma}=\frac{4e^2C_{\gamma\gamma}^{\text{eff}}}{\Lambda_{PQ}}=-\frac{\alpha}{2\pi f_a}\left(\frac{E}{N}-2.03\right) \tag{60}$$

where $\alpha=\frac{e^2}{4\pi}$. Due to the gluon-axion interaction, the axion gets a mass term, which is described at low energies as an axion–pion interaction [231]

$$m_a=5.7(7)\mu eV\left(\frac{10^{12}\text{GeV}}{f_a}\right). \tag{61}$$

References

1. G. Aad et al., Observation of a new particle in the search for the Standard Model Higgs boson with the ATLAS detector at the LHC. Phys. Lett. B **716**, 1–29 (2012)
2. S. Chatrchyan et al., Observation of a New Boson at a Mass of 125 GeV with the CMS Experiment at the LHC. Phys. Lett. B **716**, 30–61 (2012)
3. G.C. Branco, P.M. Ferreira, L. Lavoura, M.N. Rebelo, M. Sher, J.P. Silva, Theory and phenomenology of two-Higgs-doublet models. Phys. Rept. **516**, 1–102 (2012)
4. T.D. Lee, A Theory of Spontaneous T Violation. Phys. Rev. D **8**, 1226–1239 (1973)
5. H.E. Haber, G.L. Kane, The Search for Supersymmetry: Probing Physics Beyond the Standard Model. Phys. Rept. **117**, 75–263 (1985)
6. J.E. Kim, Light Pseudoscalars, Particle Physics and Cosmology. Phys. Rept. **150**, 1–177 (1987)
7. N. Turok, J. Zadrozny, Electroweak baryogenesis in the two doublet model. Nucl. Phys. B **358**, 471–493 (1991)
8. V. Barger, P. Langacker, M. McCaskey, M. Ramsey-Musolf, G. Shaughnessy, Complex Singlet Extension of the Standard Model. Phys. Rev. D **79**, 015018 (2009)
9. R.M. Schabinger, J.D. Wells, A Minimal spontaneously broken hidden sector and its impact on Higgs boson physics at the large hadron collider. Phys. Rev. D **72**, 093007 (2005)
10. C.-W. Chiang, M.J. Ramsey-Musolf, E. Senaha, Standard Model with a Complex Scalar Singlet: Cosmological Implications and Theoretical Considerations. Phys. Rev. D **97**(1), 015005 (2018)
11. J. McDonald, Gauge singlet scalars as cold dark matter. Phys. Rev. D **50**, 3637–3649 (1994)

12. L. Lopez Honorez, E. Nezri, J. F. Oliver, M. H. G. Tytgat, The Inert Doublet Model: An Archetype for Dark Matter. JCAP **02**, 028 (2007)
13. L. Lopez Honorez, C. E. Yaguna, The inert doublet model of dark matter revisited. JHEP **09**, 046 (2010)
14. M. Carena, H.E. Haber, I. Low, N.R. Shah, C.E.M. Wagner, Alignment limit of the NMSSM Higgs sector. Phys. Rev. D **93**(3), 035013 (2016)
15. S.L. Glashow, Partial Symmetries of Weak Interactions. Nucl. Phys. **22**, 579–588 (1961)
16. S. Weinberg, A Model of Leptons. Phys. Rev. Lett. **19**, 1264–1266 (1967)
17. A. Salam, Weak and Electromagnetic Interactions. Conf. Proc. C **680519**, 367–377 (1968)
18. R. Davis Jr., D.S. Harmer, K.C. Hoffman, Search for neutrinos from the sun. Phys. Rev. Lett. **20**, 1205–1209 (1968)
19. J. N. Bahcall, "Solving the mystery of the missing neutrinos," 6 (2004)
20. B. Pontecorvo, Inverse beta processes and nonconservation of lepton charge. Zh. Eksp. Teor. Fiz. **34**, 247 (1957)
21. L. Wolfenstein, Neutrino Oscillations in Matter. Phys. Rev. D **17**, 2369–2374 (1978)
22. S.P. Mikheyev, A.Y. Smirnov, Resonance amplification of oscillations in matter and spectroscopy of solar neutrinos. Sov. J. Nucl. Phys. **42**, 913–917 (1985)
23. F. Kaether, W. Hampel, G. Heusser, J. Kiko, T. Kirsten, Reanalysis of the GALLEX solar neutrino flux and source experiments. Phys. Lett. B **685**, 47–54 (2010)
24. B.T. Cleveland, T. Daily, R. Davis Jr., J.R. Distel, K. Lande, C.K. Lee, P.S. Wildenhain, J. Ullman, Measurement of the solar electron neutrino flux with the Homestake chlorine detector. Astrophys. J. **496**, 505–526 (1998)
25. B. Aharmim et al., Combined analysis of all three phases of solar neutrino data from the sudbury neutrino observatory. Phys. Rev. C **88**, 025501 (2013)
26. G. Bellini et al., Measurement of the solar 8B neutrino rate with a liquid scintillator target and 3 MeV energy threshold in the Borexino detector. Phys. Rev. D **82**, 033006 (2010)
27. G. Bellini, J. Benziger, D. Bick, G. Bonfini, D. Bravo, B. Caccianiga, L. Cadonati, F. Calaprice, A. Caminata, P. Cavalcante, A. Chavarria, A. Chepurnov, D. D'Angelo, S. Davini, A. Derbin, A. Empl, A. Etenko, K. Fomenko, D. Franco, F. Gabriele, C. Galbiati, S. Gazzana, C. Ghiano, M. Giammarchi, M. Göger-Neff, A. Goretti, M. Gromov, C. Hagner, E. Hungerford, A. Ianni, A. Ianni, V. Kobychev, D. Korablev, G. Korga, D. Kryn, M. Laubenstein, B. Lehnert, T. Lewke, E. Litvinovich, F. Lombardi, P. Lombardi, L. Ludhova, G. Lukyanchenko, I. Machulin, S. Manecki, W. Maneschg, S. Marcocci, Q. Meindl, E. Meroni, M. Meyer, L. Miramonti, M. Misiaszek, M. Montuschi, P. Mosteiro, V. Muratova, L. Oberauer, M. Obolensky, F. Ortica, K. Otis, M. Pallavicini, L. Papp, L. Perasso, A. Pocar, G. Ranucci, A. Razeto, A. Re, A. Romani, N. Rossi, R. Saldanha, C. Salvo, S. Schönert, H. Simgen, M. Skorokhvatov, O. Smirnov, A. Sotnikov, S. Sukhotin, Y. Suvorov, R. Tartaglia, G. Testera, D. Vignaud, R.B. Vogelaar, F. von Feilitzsch, H. Wang, J. Winter, M. Wojcik, A. Wright, M. Wurm, O. Zaimidoroga, S. Zavatarelli, K. Zuber, G. Zuzel, B. Collaboration, Neutrinos from the primary proton-proton fusion process in the sun. Nature **512**, 383–386 (2014)
28. J. Hosaka et al., Solar neutrino measurements in super-Kamiokande-I. Phys. Rev. D **73**, 112001 (2006)
29. J. Hosaka et al., Three flavor neutrino oscillation analysis of atmospheric neutrinos in Super-Kamiokande. Phys. Rev. D **74**, 032002 (2006)
30. M.G. Aartsen et al., Determining neutrino oscillation parameters from atmospheric muon neutrino disappearance with three years of IceCube DeepCore data. Phys. Rev. D **91**(7), 072004 (2015)
31. A. Gando et al., Constraints on θ_{13} from A Three-Flavor Oscillation Analysis of Reactor Antineutrinos at KamLAND. Phys. Rev. D **83**, 052002 (2011)
32. M. Apollonio et al., Limits on neutrino oscillations from the CHOOZ experiment. Phys. Lett. B **466**, 415–430 (1999)
33. A. Piepke, Final results from the Palo Verde neutrino oscillation experiment. Prog. Part. Nucl. Phys. **48**, 113–121 (2002)
34. F.P. An et al., New Measurement of Antineutrino Oscillation with the Full Detector Configuration at Daya Bay. Phys. Rev. Lett. **115**(11), 111802 (2015)
35. S.-B. Kim, Measurement of neutrino mixing angle Θ_{13} and mass difference Δm^2_{ee} from reactor antineutrino disappearance in the RENO experiment. Nucl. Phys. B **908**, 94–115 (2016)
36. J. Kopp, P.A.N. Machado, M. Maltoni, T. Schwetz, Sterile Neutrino Oscillations: The Global Picture. JHEP **05**, 050 (2013)
37. P. Adamson et al., Measurement of Neutrino and Antineutrino Oscillations Using Beam and Atmospheric Data in MINOS. Phys. Rev. Lett. **110**(25), 251801 (2013)
38. K. Abe et al., Observation of Electron Neutrino Appearance in a Muon Neutrino Beam. Phys. Rev. Lett. **112**, 061802 (2014)
39. P. Adamson et al., First measurement of electron neutrino appearance in NOvA. Phys. Rev. Lett. **116**(15), 151806 (2016)
40. J. Schechter, J.W.F. Valle, Neutrino Masses in SU(2) x U(1) Theories. Phys. Rev. D **22**, 2227 (1980)
41. E. Ma, U. Sarkar, Neutrino masses and leptogenesis with heavy Higgs triplets. Phys. Rev. Lett. **80**, 5716–5719 (1998)
42. R. Foot, H. Lew, X.G. He, G.C. Joshi, Seesaw Neutrino Masses Induced by a Triplet of Leptons. Z. Phys. C **44**, 441 (1989)
43. R.N. Mohapatra, J.W.F. Valle, Neutrino Mass and Baryon Number Nonconservation in Superstring Models. Phys. Rev. D **34**, 1642 (1986)
44. M.C. Gonzalez-Garcia, J.W.F. Valle, Fast Decaying Neutrinos and Observable Flavor Violation in a New Class of Majoron Models. Phys. Lett. B **216**, 360–366 (1989)
45. G.C. Branco, D. Emmanuel-Costa, M.N. Rebelo, P. Roy, Four Zero Neutrino Yukawa Textures in the Minimal Seesaw Framework. Phys. Rev. D **77**, 053011 (2008)
46. S. Choubey, W. Rodejohann, P. Roy, Phenomenological consequences of four zero neutrino Yukawa textures. Nucl. Phys. B **808**, 272–291 (2009). [Erratum: Nucl.Phys.B 818, 136–136 (2009)]
47. B. Adhikary, A. Ghosal, P. Roy, Neutrino Masses, Cosmological Bound and Four Zero Yukawa Textures. Mod. Phys. Lett. A **26**, 2427–2435 (2011)
48. B. Adhikary, A. Ghosal, P. Roy, Baryon asymmetry from leptogenesis with four zero neutrino Yukawa textures. JCAP **01**, 025 (2011)
49. G.C. Branco, M.N. Rebelo, J.I. Silva-Marcos, Leptogenesis, Yukawa textures and weak basis invariants. Phys. Lett. B **633**, 345–354 (2006)
50. J.-W. Mei, Running neutrino masses, leptonic mixing angles and CP-violating phases: From M(Z) to Lambda(GUT). Phys. Rev. D **71**, 073012 (2005)
51. C. Hagedorn, J. Kersten, M. Lindner, Stability of texture zeros under radiative corrections in see-saw models. Phys. Lett. B **597**, 63–72 (2004)
52. S. Antusch, J. Kersten, M. Lindner, M. Ratz, M.A. Schmidt, Running neutrino mass parameters in see-saw scenarios. JHEP **03**, 024 (2005)
53. P. O. Ludl, W. Grimus, A complete survey of texture zeros in the lepton mass matrices. JHEP **07**, 090 (2014). [Erratum: JHEP 10, 126 (2014)]
54. P.M. Ferreira, L. Lavoura, New textures for the lepton mass matrices. Nucl. Phys. B **891**, 378–400 (2015)
55. P.O. Ludl, W. Grimus, A complete survey of texture zeros in general and symmetric quark mass matrices. Phys. Lett. B **744**, 38–42 (2015)

56. W. Grimus, A.S. Joshipura, L. Lavoura, M. Tanimoto, Symmetry realization of texture zeros. Eur. Phys. J. C **36**, 227–232 (2004)
57. R.M. Fonseca, W. Grimus, Classification of lepton mixing matrices from finite residual symmetries. JHEP **09**, 033 (2014)
58. Y. Giraldo, R. Martinez, E. Rojas, J.C. Salazar, Flavored axions and the flavor problem. Eur. Phys. J. C **82**(12), 1131 (2022)
59. F. Björkeroth, L. Di Luzio, F. Mescia, E. Nardi, $U(1)$ flavour symmetries as Peccei-Quinn symmetries. JHEP **02**, 133 (2019)
60. T.P. Cheng, M. Sher, Mass Matrix Ansatz and Flavor Nonconservation in Models with Multiple Higgs Doublets. Phys. Rev. D **35**, 3484 (1987)
61. K. Matsuda, H. Nishiura, Can four-zero-texture mass matrix model reproduce the quark and lepton mixing angles and CP violating phases? Phys. Rev. D **74**, 033014 (2006)
62. A. E. Carcamo Hernandez, R. Martinez, J. A. Rodriguez, Different kind of textures of Yukawa coupling matrices in the two Higgs doublet model type III. Eur. Phys. J. C **50**, 935–948 (2007)
63. P. Langacker, M. Plumacher, Flavor changing effects in theories with a heavy Z' boson with family nonuniversal couplings. Phys. Rev. D **62**, 013006 (2000)
64. K. Leroux, D. London, Flavor changing neutral currents and leptophobic Z' gauge bosons. Phys. Lett. B **526**, 97–103 (2002)
65. S.F. King, S. Moretti, R. Nevzorov, Theory and phenomenology of an exceptional supersymmetric standard model. Phys. Rev. D **73**, 035009 (2006)
66. C. Alvarado, R. Martinez, F. Ochoa, Quark mass hierarchy in 3-3-1 models. Phys. Rev. D **86**, 025027 (2012)
67. L.E. Ibanez, G.G. Ross, Fermion masses and mixing angles from gauge symmetries. Phys. Lett. B **332**, 100–110 (1994)
68. P. Binetruy, P. Ramond, Yukawa textures and anomalies. Phys. Lett. B **350**, 49–57 (1995)
69. Y. Nir, Gauge unification, Yukawa hierarchy and the mu problem. Phys. Lett. B **354**, 107–110 (1995)
70. V. Jain, R. Shrock, Models of fermion mass matrices based on a flavor dependent and generation dependent U(1) gauge symmetry. Phys. Lett. B **352**, 83–91 (1995)
71. E. Dudas, S. Pokorski, C.A. Savoy, Yukawa matrices from a spontaneously broken Abelian symmetry. Phys. Lett. B **356**, 45–55 (1995)
72. F. Pisano, V. Pleitez, An SU(3) x U(1) model for electroweak interactions. Phys. Rev. D **46**, 410–417 (1992)
73. P.H. Frampton, Chiral dilepton model and the flavor question. Phys. Rev. Lett. **69**, 2889–2891 (1992)
74. R. Foot, H.N. Long, T.A. Tran, $SU(3)_L \otimes U(1)_N$ and $SU(4)_L \otimes U(1)_N$ gauge models with right-handed neutrinos. Phys. Rev. D **50**(1), R34–R38 (1994)
75. H.N. Long, The 331 model with right handed neutrinos. Phys. Rev. D **53**, 437–445 (1996)
76. H.N. Long, SU(3)-L x U(1)-N model for right-handed neutrino neutral currents. Phys. Rev. D **54**, 4691–4693 (1996)
77. H.N. Long, Scalar sector of the 3 3 1 model with three Higgs triplets. Mod. Phys. Lett. A **13**, 1865–1874 (1998)
78. R.A. Diaz, R. Martinez, J.A. Rodriguez, A New supersymmetric SU(3)(L) x U(1)(X) gauge model. Phys. Lett. B **552**, 287–292 (2003)
79. R.A. Diaz, R. Martinez, F. Ochoa, The Scalar sector of the SU(3)(c) x SU(3)(L) x U(1)(X) model. Phys. Rev. D **69**, 095009 (2004)
80. R.A. Diaz, R. Martinez, F. Ochoa, SU(3)(c) x SU(3)(L) x U(1)(X) models for beta arbitrary and families with mirror fermions. Phys. Rev. D **72**, 035018 (2005)
81. F. Ochoa, R. Martinez, Family dependence in SU(3)(c) x SU(3)(L) x U(1)(X) models. Phys. Rev. D **72**, 035010 (2005)
82. S.M. Barr, Light Fermion Mass Hierarchy and Grand Unification. Phys. Rev. D **21**, 1424 (1980)
83. T.R. Taylor, G. Veneziano, Quenching the Cosmological Constant. Phys. Lett. B **228**, 311–316 (1989)
84. S.M. Barr, A Simple and Predictive Model for Quark and Lepton Masses. Phys. Rev. Lett. **64**, 353 (1990)
85. S. Weinberg, Electromagnetic and weak masses. Phys. Rev. Lett. **29**, 388–392 (1972)
86. R.N. Mohapatra, Gauge Model for Chiral Symmetry Breaking and Muon electron Mass Ratio. Phys. Rev. D **9**, 3461 (1974)
87. S.M. Barr, A. Zee, A New Approach to the electron-Muon Mass Ratio. Phys. Rev. D **15**, 2652 (1977)
88. B.S. Balakrishna, Fermion Mass Hierarchy From Radiative Corrections. Phys. Rev. Lett. **60**, 1602 (1988)
89. S.M. Barr, Flavor without flavor symmetry. Phys. Rev. D **65**, 096012 (2002)
90. L. Ferretti, S.F. King, A. Romanino, Flavour from accidental symmetries. JHEP **11**, 078 (2006)
91. S.M. Barr, Doubly Lopsided Mass Matrices from Unitary Unification. Phys. Rev. D **78**, 075001 (2008)
92. P.H. Frampton, T.W. Kephart, Fermion Mixings in SU(9) Family Unification. Phys. Lett. B **681**, 343–346 (2009)
93. K.S. Babu, S.M. Barr, Large neutrino mixing angles in unified theories. Phys. Lett. B **381**, 202–208 (1996)
94. J. Sato, T. Yanagida, Large lepton mixing in a coset space family unification on E(7) / SU(5) x U(1)**3. Phys. Lett. B **430**, 127–131 (1998)
95. N. Irges, S. Lavignac, P. Ramond, Predictions from an anomalous U(1) model of Yukawa hierarchies. Phys. Rev. D **58**, 035003 (1998)
96. S.M. Barr, I. Dorsner, A General classification of three neutrino models and U(e3). Nucl. Phys. B **585**, 79–104 (2000)
97. N. Haba, H. Murayama, Anarchy and hierarchy. Phys. Rev. D **63**, 053010 (2001)
98. X.-G. He, Y.-Y. Keum, R.R. Volkas, A(4) flavor symmetry breaking scheme for understanding quark and neutrino mixing angles. JHEP **04**, 039 (2006)
99. Y.H. Ahn, S.K. Kang, C.S. Kim, Spontaneous CP Violation in A_4 Flavor Symmetry and Leptogenesis. Phys. Rev. D **87**(11), 113012 (2013)
100. R. González Felipe, H. Serôdio, J. P. Silva, Models with three Higgs doublets in the triplet representations of A_4 or S_4. Phys. Rev. D **87**(5), 055010 (2013)
101. H. Ishimori, E. Ma, New Simple A_4 Neutrino Model for Nonzero θ_{13} and Large δ_{CP}. Phys. Rev. D **86**, 045030 (2012)
102. F. Gonzalez Canales, A. Mondragon, M. Mondragon, The S_3 Flavour Symmetry: Neutrino Masses and Mixings. Fortsch. Phys. **61**, 546–570 (2013)
103. R.N. Mohapatra, C.C. Nishi, S_4 Flavored CP Symmetry for Neutrinos. Phys. Rev. D **86**, 073007 (2012)
104. G.-J. Ding, S.F. King, C. Luhn, A.J. Stuart, Spontaneous CP violation from vacuum alignment in S_4 models of leptons. JHEP **05**, 084 (2013)
105. E. Ma, Neutrino Mixing and Geometric CP Violation with Delta(27) Symmetry. Phys. Lett. B **723**, 161–163 (2013)
106. C.C. Nishi, Generalized CP symmetries in $\Delta(27)$ flavor models. Phys. Rev. D **88**(3), 033010 (2013)
107. G. Altarelli, F. Feruglio, Tri-bimaximal neutrino mixing from discrete symmetry in extra dimensions. Nucl. Phys. B **720**, 64–88 (2005)
108. H. Ishimori, Y. Shimizu, M. Tanimoto, A. Watanabe, Neutrino masses and mixing from S_4 flavor twisting. Phys. Rev. D **83**, 033004 (2011)
109. A. Kadosh, E. Pallante, An A(4) flavor model for quarks and leptons in warped geometry. JHEP **08**, 115 (2010)
110. G.-J. Ding, Y.-L. Zhou, Dirac Neutrinos with S_4 Flavor Symmetry in Warped Extra Dimensions. Nucl. Phys. B **876**, 418–452 (2013)

111. Y. Giraldo, Texture Zeros and WB Transformations in the Quark Sector of the Standard Model. Phys. Rev. D **86**, 093021 (2012)
112. G. C. Branco, D. Emmanuel-Costa, R. Gonzalez Felipe, Texture zeros and weak basis transformations. Phys. Lett. B **477**, 147–155 (2000)
113. Y. Giraldo, E. Rojas, CKM mixings from mass matrices with five texture zeros. Phys. Rev. D **104**(7), 075009 (2021)
114. P. Ramond, R.G. Roberts, G.G. Ross, Stitching the Yukawa quilt. Nucl. Phys. B **406**, 19–42 (1993)
115. H. Fritzsch, Z.-Z. Xing, Mass and flavor mixing schemes of quarks and leptons. Prog. Part. Nucl. Phys. **45**, 1–81 (2000)
116. G.C. Branco, L. Lavoura, F. Mota, Nearest Neighbor Interactions and the Physical Content of Fritzsch Mass Matrices. Phys. Rev. D **39**, 3443 (1989)
117. X.-G. He, W.-S. Hou, Relating the Long B Lifetime to a Very Heavy Top Quark. Phys. Rev. D **41**, 1517 (1990)
118. H. Fritzsch, Weak Interaction Mixing in the Six - Quark Theory. Phys. Lett. B **73**, 317–322 (1978)
119. H. Fritzsch, Calculating the Cabibbo Angle. Phys. Lett. B **70**, 436–440 (1977)
120. H. Fritzsch, Quark Masses and Flavor Mixing. Nucl. Phys. B **155**, 189–207 (1979)
121. D.-S. Du, Z.-Z. Xing, A Modified Fritzsch ansatz with additional first order perturbation. Phys. Rev. D **48**, 2349–2352 (1993)
122. H. Fritzsch, Z.-Z. Xing, Four zero texture of Hermitian quark mass matrices and current experimental tests. Phys. Lett. B **555**, 63–70 (2003)
123. R. L. Workman et al., Review of Particle Physics. PTEP **2022**, 083C01 (2022)
124. Z.-Z. Xing, H. Zhang, Complete parameter space of quark mass matrices with four texture zeros. J. Phys. G **30**, 129–136 (2004)
125. Y.-F. Zhou, Textures and hierarchies in quark mass matrices with four texture zeros 9 (2003)
126. R. H. Benavides, Y. Giraldo, L. Mu noz, W. A. Ponce, E. Rojas, Five Texture Zeros for Dirac Neutrino Mass Matrices. J. Phys. G, **47**(11), 115002 (2020)
127. Y. Giraldo, Seeking Texture Zeros in the Quark Mass Matrix Sector of the Standard Model. Nucl. Part. Phys. Proc. **267–269**, 76–78 (2015)
128. F. Wilczek, Axions and family symmetry breaking. Phys. Rev. Lett. **49**, 1549–1552 (1982)
129. L. Calibbi, F. Goertz, D. Redigolo, R. Ziegler, J. Zupan, Minimal axion model from flavor. Phys. Rev. D **95**(9), 095009 (2017)
130. C.Q. Geng, J.N. Ng, Flavor Connections and Neutrino Mass Hierarchy Invariant Invisible Axion Models Without Domain Wall Problem. Phys. Rev. D **39**, 1449 (1989)
131. Z.G. Berezhiani, M.Y. Khlopov, Cosmology of Spontaneously Broken Gauge Family Symmetry. Z. Phys. C **49**, 73–78 (1991)
132. M. Hindmarsh, P. Moulatsiotis, Constraints on variant axion models. Phys. Rev. D **56**, 8074–8081 (1997)
133. Y. Giraldo, R. Martínez, E. Rojas, J. C. Salazar, A minimal axion model for mass matrices with five texture-zeros. **4** (2023)
134. F. Björkeroth, E.J. Chun, S.F. King, Flavourful Axion Phenomenology. JHEP **08**, 117 (2018)
135. M. Reig, J.W.F. Valle, F. Wilczek, SO(3) family symmetry and axions. Phys. Rev. D **98**(9), 095008 (2018)
136. M. Linster, R. Ziegler, A Realistic $U(2)$ Model of Flavor. JHEP **08**, 058 (2018)
137. Y.H. Ahn, Compact model for Quarks and Leptons via flavored-Axions. Phys. Rev. D **98**(3), 035047 (2018)
138. F. Arias-Aragon, L. Merlo, The minimal flavour violating axion. JHEP **10**, 168 (2017). [Erratum: JHEP 11, 152 (2019)]
139. Y. Ema, K. Hamaguchi, T. Moroi, K. Nakayama, Flaxion: a minimal extension to solve puzzles in the standard model. JHEP **01**, 096 (2017)
140. T. Alanne, S. Blasi, F. Goertz, Common source for scalars: Flavored axion-Higgs unification. Phys. Rev. D **99**(1), 015028 (2019)
141. S. Bertolini, L. Di Luzio, H. Kolešová, M. Malinský, Massive neutrinos and invisible axion minimally connected. Phys. Rev. D **91**(5), 055014 (2015)
142. A. Celis, J. Fuentes-Martín, H. Serôdio, A class of invisible axion models with FCNCs at tree level. JHEP **12**, 167 (2014)
143. Y.H. Ahn, Flavored Peccei-Quinn symmetry. Phys. Rev. D **91**, 056005 (2015)
144. C. Cheung, Axion Protection from Flavor. JHEP **06**, 074 (2010)
145. M.E. Albrecht, T. Feldmann, T. Mannel, Goldstone Bosons in Effective Theories with Spontaneously Broken Flavour Symmetry. JHEP **10**, 089 (2010)
146. T. Appelquist, Y. Bai, M. Piai, SU(3) Family Gauge Symmetry and the Axion. Phys. Rev. D **75**, 073005 (2007)
147. R.D. Peccei, H.R. Quinn, CP Conservation in the Presence of Instantons. Phys. Rev. Lett. **38**, 1440–1443 (1977)
148. R.D. Peccei, H.R. Quinn, Constraints Imposed by CP Conservation in the Presence of Instantons. Phys. Rev. D **16**, 1791–1797 (1977)
149. S. Weinberg, A New Light Boson? Phys. Rev. Lett. **40**, 223–226 (1978)
150. F. Wilczek, Problem of Strong P and T Invariance in the Presence of Instantons. Phys. Rev. Lett. **40**, 279–282 (1978)
151. J.E. Kim, Weak Interaction Singlet and Strong CP Invariance. Phys. Rev. Lett. **43**, 103 (1979)
152. M.S. Turner, Windows on the Axion. Phys. Rept. **197**, 67–97 (1990)
153. G.G. Raffelt, Astrophysical methods to constrain axions and other novel particle phenomena. Phys. Rept. **198**, 1–113 (1990)
154. J. Preskill, M.B. Wise, F. Wilczek, Cosmology of the Invisible Axion. Phys. Lett. B **120**, 127–132 (1983)
155. L.F. Abbott, P. Sikivie, A Cosmological Bound on the Invisible Axion. Phys. Lett. B **120**, 133–136 (1983)
156. M. Dine, W. Fischler, The Not So Harmless Axion. Phys. Lett. B **120**, 137–141 (1983)
157. M.A. Shifman, A.I. Vainshtein, V.I. Zakharov, Can Confinement Ensure Natural CP Invariance of Strong Interactions? Nucl. Phys. B **166**, 493–506 (1980)
158. M. Dine, W. Fischler, M. Srednicki, A Simple Solution to the Strong CP Problem with a Harmless Axion. Phys. Lett. B **104**, 199–202 (1981)
159. A.R. Zhitnitsky, On Possible Suppression of the Axion Hadron Interactions. (In Russian). Sov. J. Nucl. Phys. **31**, 260 (1980)
160. L. Di Luzio, M. Giannotti, E. Nardi, L. Visinelli, The landscape of QCD axion models. Phys. Rept. **870**, 1–117 (2020)
161. N. Viaux, M. Catelan, P.B. Stetson, G. Raffelt, J. Redondo, A.A.R. Valcarce, A. Weiss, Neutrino and axion bounds from the globular cluster M5 (NGC 5904). Phys. Rev. Lett. **111**, 231301 (2013)
162. E. Arik et al., Probing eV-scale axions with CAST. JCAP **02**, 008 (2009)
163. Y. Inoue, Y. Akimoto, R. Ohta, T. Mizumoto, A. Yamamoto, M. Minowa, Search for solar axions with mass around 1 eV using coherent conversion of axions into photons. Phys. Lett. B **668**, 93–97 (2008)
164. M. M. Miller Bertolami, B. E. Melendez, L. G. Althaus, J. Isern, Revisiting the axion bounds from the Galactic white dwarf luminosity function. JCAP **10**, 069 (2014)
165. M. Giannotti, I.G. Irastorza, J. Redondo, A. Ringwald, K. Saikawa, Stellar Recipes for Axion Hunters. JCAP **10**, 010 (2017)
166. J. Isern, E. García-Berro, S. Torres, R. Cojocaru, S. Catalán, Axions and the luminosity function of white dwarfs: the thin and thick discs, and the halo. Mon. Not. R. Astron. Soc. **478**, 2569–2575 (2018)

167. O. Straniero, I. Dominguez, M. Giannotti, and A. Mirizzi, Axion-electron coupling from the RGB tip of Globular Clusters (2018). arXiv e-prints, p. arXiv:1802.10357
168. R. Verma, Exploring the predictability of symmetric texture zeros in quark mass matrices. Phys. Rev. D **96**(9), 093010 (2017)
169. Z.-Z. Xing, Flavor structures of charged fermions and massive neutrinos. Phys. Rept. **854**, 1–147 (2020)
170. B.R. Desai, A.R. Vaucher, Quark mass matrices with four and five texture zeroes, and the CKM matrix, in terms of mass eigenvalues. Phys. Rev. D **63**, 113001 (2001)
171. W.A. Ponce, J.D. Gómez, R.H. Benavides, Five texture zeros and CP violation for the standard model quark mass matrices. Phys. Rev. D **87**(5), 053016 (2013)
172. Y. Giraldo, E. Rojas, Five Non-Fritzsch Texture Zeros for Quarks Mass Matrices in the Standard Model. in 38th International Symposium on Physics in Collision, 11 (2018)
173. C. Hagedorn, W. Rodejohann, Minimal mass matrices for dirac neutrinos. JHEP **07**, 034 (2005)
174. G. Ahuja, M. Gupta, M. Randhawa, R. Verma, Texture specific mass matrices with Dirac neutrinos and their implications. Phys. Rev. D **79**, 093006 (2009)
175. X.-W. Liu, S. Zhou, Texture Zeros for Dirac Neutrinos and Current Experimental Tests. Int. J. Mod. Phys. A **28**, 1350040 (2013)
176. R. Verma, Lower bound on neutrino mass and possible CP violation in neutrino oscillations. Phys. Rev. D **88**, 111301 (2013)
177. R. Verma, Lepton textures and neutrino oscillations. Int. J. Mod. Phys. A **29**(21), 1444009 (2014)
178. P. Fakay, S. Sharma, G. Ahuja, M. Gupta, Leptonic mixing angle θ_{13} and ruling out of minimal texture for Dirac neutrinos. PTEP **2014**(2), 023B03 (2014)
179. L.M. Cebola, D. Emmanuel-Costa, R.G. Felipe, Confronting predictive texture zeros in lepton mass matrices with current data. Phys. Rev. D **92**(2), 025005 (2015)
180. R.R. Gautam, M. Singh, M. Gupta, Neutrino mass matrices with one texture zero and a vanishing neutrino mass. Phys. Rev. D **92**(1), 013006 (2015)
181. G. Ahuja, S. Sharma, P. Fakay, M. Gupta, General lepton textures and their implications. Mod. Phys. Lett. A **30**(34), 1530025 (2015)
182. M. Singh, Texture One Zero Dirac Neutrino Mass Matrix With Vanishing Determinant or Trace Condition. Nucl. Phys. B **931**, 446–468 (2018)
183. G. Ahuja, M. Gupta, Texture zero mass matrices and nature of neutrinos. Int. J. Mod. Phys. A **33**(31), 1844032 (2018)
184. J. Barranco, D. Delepine, L. Lopez-Lozano, Neutrino Mass Determination from a Four-Zero Texture Mass Matrix. Phys. Rev. D **86**, 053012 (2012)
185. Y.A. Garnica, S.F. Mantilla, R. Martinez, H. Vargas, From Peccei Quinn symmetry to mass hierarchy problem. J. Phys. G **48**(9), 095002 (2021)
186. A. Ringwald, K. Saikawa, Axion dark matter in the post-inflationary Peccei-Quinn symmetry breaking scenario. Phys. Rev. D 93(8), 085031 (2016). [Addendum: Phys.Rev.D 94, 049908 (2016)]
187. I. Brivio, M.B. Gavela, L. Merlo, K. Mimasu, J.M. No, R. del Rey, V. Sanz, ALPs Effective Field Theory and Collider Signatures. Eur. Phys. J. C **77**(8), 572 (2017)
188. R. H. Benavides, D. V. Forero, L. Mu noz, J. M. Mu noz, A. Rico, A. Tapia, Five texture zeros in the lepton sector and neutrino oscillations at DUNE. Phys. Rev. D **107**(3), 036008 (2023)
189. H. Georgi, D.B. Kaplan, L. Randall, Manifesting the Invisible Axion at Low-energies. Phys. Lett. B **169**, 73–78 (1986)
190. M.B. Gavela, R. Houtz, P. Quilez, R. Del Rey, O. Sumensari, Flavor constraints on electroweak ALP couplings. Eur. Phys. J. C **79**(5), 369 (2019)
191. M. Bauer, M. Neubert, A. Thamm, Collider Probes of Axion-Like Particles. JHEP **12**, 044 (2017)
192. A. Salvio, A. Strumia, W. Xue, Thermal axion production. JCAP **01**, 011 (2014)
193. E. Cortina Gil et al. Measurement of the very rare $K^+ \to \pi^+ \nu\bar{\nu}$ decay. JHEP **06**, 093 (2021)
194. R.D. Bolton et al., Search for rare Muon decays with the crystal box detector. Phys. Rev. D **38**, 2077 (1988)
195. A. Jodidio, B. Balke, J. Carr, G. Gidal, K.A. Shinsky, H.M. Steiner, D.P. Stoker, M. Strovink, R.D. Tripp, B. Gobbi, C.J. Oram, Erratum: Search for right-handed currents in muon decay [phys. rev. d 34, 1967 (1986)]. Phys. Rev. D **37**, 237–238 (1988)
196. R. Bayes et al., Search for two body muon decay signals. Phys. Rev. D **91**(5), 052020 (2015)
197. H. Albrecht et al., A Search for lepton flavor violating decays tau –> e alpha, tau –> mu alpha. Z. Phys. C **68**, 25–28 (1995)
198. H. Georgi, D.V. Nanopoulos, Suppression of Flavor Changing Effects From Neutral Spinless Meson Exchange in Gauge Theories. Phys. Lett. B **82**, 95–96 (1979)
199. C. O'Hare, cajohare/axionlimits: Axionlimits. https://cajohare.github.io/AxionLimits/ (2020)
200. S. Chaudhuri, P.W. Graham, K. Irwin, J. Mardon, S. Rajendran, Y. Zhao, Radio for hidden-photon dark matter detection. Phys. Rev. D **92**(7), 075012 (2015)
201. D. Alesini, D. Babusci, D. Di Gioacchino, C. Gatti, G. Lamanna, C. Ligi, The KLASH proposal. **7** (2017)
202. C. Gatti et al. The Klash Proposal: Status and Perspectives. in 14th Patras Workshop on Axions, WIMPs and WISPs, 11 (2018)
203. I. Stern, ADMX Status. PoS ICHEP2016, 198 (2016)
204. M. Lawson, A.J. Millar, M. Pancaldi, E. Vitagliano, F. Wilczek, Tunable axion plasma haloscopes. Phys. Rev. Lett. **123**(14), 141802 (2019)
205. S. Beurthey et al., "MADMAX Status Report," 3 (2020)
206. E. Armengaud et al., Conceptual Design of the International Axion Observatory (IAXO). JINST **9**, T05002 (2014)
207. I. Shilon, A. Dudarev, H. Silva, U. Wagner, H.H.J. ten Kate, New Superconducting Toroidal Magnet System for IAXO, the International AXion Observatory. AIP Conf. Proc. **1573**(1), 1559–1566 (2015)
208. J.L. Ouellet et al., First Results from ABRACADABRA-10 cm: A Search for Sub-μeV Axion Dark Matter. Phys. Rev. Lett. **122**(12), 121802 (2019)
209. C. Bartram et al. Search for Invisible Axion Dark Matter in the 3.3–4.2 μeV Mass Range. Phys. Rev. Lett. 127(26), 261803 (2021)
210. T. Braine et al., Extended Search for the Invisible Axion with the Axion Dark Matter Experiment. Phys. Rev. Lett. **124**(10), 101303 (2020)
211. C. Bartram et al., Axion dark matter experiment: Run 1B analysis details. Phys. Rev. D **103**(3), 032002 (2021)
212. V. Anastassopoulos et al., New CAST Limit on the Axion-Photon Interaction. Nature Phys. **13**, 584–590 (2017)
213. S. Andriamonje et al., An Improved limit on the axion-photon coupling from the CAST experiment. JCAP **04**, 010 (2007)
214. S. Lee, S. Ahn, J. Choi, B. R. Ko, Y. K. Semertzidis, Axion Dark Matter Search around 6.7 μeV. Phys. Rev. Lett. **124**(10), 101802 (2020)
215. J. Jeong, S. Youn, S. Bae, J. Kim, T. Seong, J.E. Kim, Y.K. Semertzidis, Search for Invisible Axion Dark Matter with a Multiple-Cell Haloscope. Phys. Rev. Lett. **125**(22), 221302 (2020)
216. O. Kwon et al., First Results from an Axion Haloscope at CAPP around 10.7 μeV. Phys. Rev. Lett. **126**(19), 191802 (2021)
217. K.M. Backes et al., A quantum-enhanced search for dark matter axions. Nature **590**(7845), 238–242 (2021)
218. L. Zhong et al., Results from phase 1 of the HAYSTAC microwave cavity axion experiment. Phys. Rev. D **97**(9), 092001 (2018)
219. P. Gondolo, G.G. Raffelt, Solar neutrino limit on axions and keV-mass bosons. Phys. Rev. D **79**, 107301 (2009)

220. A. Ayala, I. Domínguez, M. Giannotti, A. Mirizzi, O. Straniero, Revisiting the bound on axion-photon coupling from Globular Clusters. Phys. Rev. Lett. **113**(19), 191302 (2014)
221. M. Regis, M. Taoso, D. Vaz, J. Brinchmann, S.L. Zoutendijk, N.F. Bouché, M. Steinmetz, Searching for light in the darkness: Bounds on ALP dark matter with the optical MUSE-faint survey. Phys. Lett. B **814**, 136075 (2021)
222. D. Grin, G. Covone, J.-P. Kneib, M. Kamionkowski, A. Blain, E. Jullo, A Telescope Search for Decaying Relic Axions. Phys. Rev. D **75**, 105018 (2007)
223. V. Prasolov, *Problems and theorems in linear algebra* (American Mathematical Society, USA, 1944)
224. S. Hassani, *Mathematical Physics: A Modern Introduction to Its Foundations* (Springer International Publishing, USA, 2013)
225. Z.-Z. Xing, Z.-H. Zhao, On the four-zero texture of quark mass matrices and its stability. Nucl. Phys. B **897**, 302–325 (2015)
226. M. Gupta, G. Ahuja, Flavor mixings and textures of the fermion mass matrices. Int. J. Mod. Phys. A **27**, 1230033 (2012)
227. H. Fusaoka, Y. Koide, Updated estimate of running quark masses. Phys. Rev. D **57**, 3986–4001 (1998)
228. J. Cardozo, J. H. Mu noz, N. Quintero, E. Rojas, Analysing the charged scalar boson contribution to the charged-current B meson anomalies. J. Phys. G **48**(3), 035001 (2021)
229. I. Esteban, M.C. Gonzalez-Garcia, A. Hernandez-Cabezudo, M. Maltoni, T. Schwetz, Global analysis of three-flavour neutrino oscillations: synergies and tensions in the determination of θ_{23}, δ_{CP}, and the mass ordering. JHEP **01**, 106 (2019)
230. G. Alonso-Álvarez, M.B. Gavela, P. Quilez, Axion couplings to electroweak gauge bosons. Eur. Phys. J. C **79**(3), 223 (2019)
231. G. Grilli di Cortona, E. Hardy, J. Pardo Vega, G. Villadoro, The QCD axion, precisely. JHEP **01**, 034 (2016)